JACC: BASIC TO TRANSLATIONAL SCIENCE VOL. 11, NO. 3, 2026

ORIGINAL RESEARCH - PRECLINICAL

HDL Regulates TGFβ-Receptor Lipid Raft Partitioning, Restoring Contractile Features of Cholesterol-Loaded Vascular Smooth Muscle Cells

Prashanth Thevkar Nagesh, PhD,[a,b,*] Shruti Rawal, PhD,[a,*] Hitoo Nishi, PhD,[a,†] Tarik Zahr, BS,[a] Joseph M. Miano, PhD,[c] Mary Sorci-Thomas, PhD,[d] Hao Xu, PhD,[d] Naveed Akbar, PhD,[e,f] Robin P. Choudhury, DM,[e,f] Mark W. Feinberg, MD,[g] Ashish Misra, PhD,[h,i] Edward A. Fisher, MD, PhD[a]

VISUAL ABSTRACT

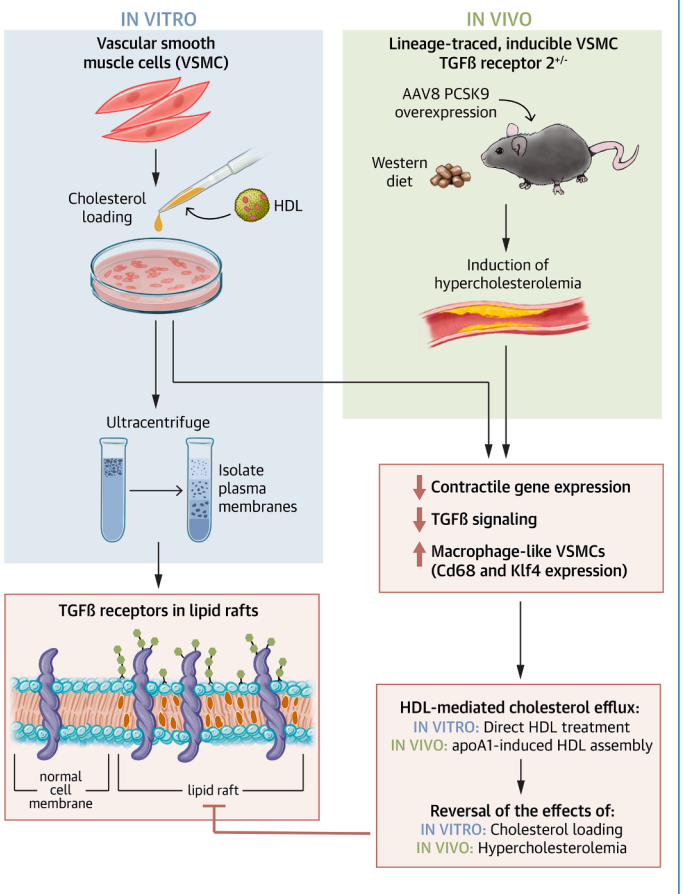

Nagesh PT, et al. JACC Basic Transl Sci. 2026;11(3):101461.

HIGHLIGHTS

- **In coronary artery hVSMCs cholesterol-loading down-regulates TGFβ signaling and its downstream target *Mir145*, resulting in loss of contractile state and gain in macrophage-like state.**
- **Cholesterol induced down-regulation of TGFβ signaling is due to localization of receptors TGFβR1 and TGFβR2 into membrane lipid rafts. HDL-mediated cholesterol efflux displaced the receptors from lipid rafts, restored TGFβ signaling and *Mir145* expression, which resulted in restoring the hVSMC contractile state.**
- **In a mouse model of atherosclerosis in which VSMCs are partially deficient in TGFβR2, infusion of ApoA1 (which forms HDL) increased the ratio of contractile to macrophage marker expression, with evidence of increased TGFβ signaling.**

From the [a]Department of Medicine, Division of Cardiology, and Cardiovascular Research Center, New York University Grossman School of Medicine, New York, New York, USA; [b]Department of Microbiology, New York University Grossman School of Medicine, New York, New York, USA; [c]Vascular Biology Center, Medical College of Georgia at Augusta University, Augusta, Georgia, USA; [d]Department of Medicine, Medical College of Wisconsin, Milwaukee, Wisconsin, USA; [e]Division of Cardiovascular Medicine,

ISSN 2452-302X https://doi.org/10.1016/j.jacbts.2025.101461

ABBREVIATIONS AND ACRONYMS

BSA = bovine serum albumin

CTB = cholera toxin B

DAPI = 4',6-diamidino-2-phenylindole

EV = extracellular vesicle

GFP$^+$ = smooth muscle cells lineage-positive

HDL = high-density lipoprotein

hVSMC = human vascular smooth muscle cell

mRNA = messenger RNA

mVSMC = mouse vascular smooth muscle cell

PBS = phosphate-buffered saline

qPCR = quantitative polymerase change reaction

siRNA = small, interfering RNA

SMA = smooth muscle actin

VSMC = vascular smooth muscle cell

SUMMARY

Many cells identified as macrophage-like in human and mouse atherosclerotic plaques are thought to be of vascular smooth muscle cell (VSMC) origin. We identified cholesterol-mediated down-regulation of TGFβ signaling in vitro in human (h)VSMCs by localization of TGFβ receptors in membrane lipid rafts, which was reversed by high-density lipoprotein (HDL)-mediated cholesterol efflux. This restored VSMC contractile marker (*Acta2*) and suppressed macrophage marker (CD68) expression by promoting TGFβ enhancement of *Mir145* expression. In vivo, administration of ApoA1 (which forms HDL) to atherosclerotic mice also promoted VSMC *Acta2* expression and reduced CD68 expression. Because macrophage-like VSMCs are thought to have adverse properties, our studies not only show mechanistically how cholesterol causes their transition, but also suggest that efflux-competent HDL particles may have a therapeutic role by restoring a more favorable phenotypic state of VSMCs in atherosclerotic plaques. (JACC Basic Transl Sci. 2026;11:101461)

Atherosclerosis is a chronic inflammatory disease characterized by accumulation of lipid-laden foam cells in arteries.[1,2] Despite advances in therapies in treating cardiovascular disease, residual risk remains with rupture of advanced atherosclerotic plaques, which leads to myocardial infarctions and strokes. Preclinical atherosclerosis research has predominantly focused on preventing plaque progression through reducing the number or inflammatory state of intraplaque monocyte-derived macrophages.[3-5] There has been increasing attention to vascular smooth muscle cells (VSMCs) as recent studies have extended understanding of their robust plasticity to the molecular level. Classically, it has been believed that VSMCs, in addition to their contractile function in the arterial media, are also atheroprotective in the plaque intima by forming a fibrous cap to prevent rupture, in contrast to intimal macrophages, which during plaque progression, have a number of adverse effects, including foam cell formation, promotion of inflammation, and expansion of the necrotic core.[6]

The distinction between "protective" and "detrimental" plaque cell types, however, has blurred with the development of lineage tracing and single-cell RNA-sequencing techniques. As noted, VSMCs can assume multiple phenotypes.[7-9] Current understanding is that intimal VSMCs derive from a subset of cells that clonally expand from the medial wall to assume a subendothelial position.[10,11] As the plaque progresses, these protective fibrous cap cells lose their expression of typical VSMC contractile genes (such as *Acta2*, *Tagln*, *Myh11*), migrate into the intima and adopt phenotypes of various other cell types, including macrophages.[12] It is not known yet whether this plastic nature of VSMC-derived cells can be influenced to stabilize the atherosclerotic plaque and prevent rupture, nor is it known what the signals are that dynamically regulate VSMC phenotype transitions during atherogenesis.

With regard to the potential signals, the TGFβ signaling pathway is of particular interest because of its well-known role in VSMC differentiation.[13] TGFβ receptor signaling is activated by the binding of TGFβ ligands to a heteromeric receptor complex composed of TGFβR1 and TGFβR2.[13] Activation of TGFβR1 leads to the phosphorylation of SMAD2 and SMAD3, which form a complex with SMAD4, which then migrates to the nucleus to influence the expression of contractile VSMC target genes, such as *Acta2*.[14,15] We were struck by the report that the conditional deletion of TGFβ

Radcliffe Department of Medicine, University of Oxford, Oxford, United Kingdom; [f]Oxford University Hospitals, National Health Service Trust, John Radcliffe Hospital, Oxford, United Kingdom; [g]Department of Medicine, Cardiovascular Division, Brigham and Women's Hospital, Harvard Medical School, Boston, Massachusetts, USA; [h]Heart Research Institute, Sydney, New South Wales, Australia; and the [i]Faculty of Medicine and Health, The University of Sydney, New South Wales, Australia. *These authors are joint first authors. †Deceased.

The authors attest they are in compliance with human studies committees and animal welfare regulations of the authors' institutions and Food and Drug Administration guidelines, including patient consent where appropriate. For more information, visit the Author Center.

Manuscript received October 25, 2023; revised manuscript received December 8, 2025, accepted December 15, 2025.

signaling in VSMCs promoted phenotypic switching in an aortic aneurysm mouse model, with the appearance of cells of VSMC origin expressing macrophage markers.[16] Taken with the finding in lung epithelial cells that cholesterol treatment increased accumulation of TGFβR1 and TGFβR2 in plasma membrane domains enriched in cholesterol (ie, lipid rafts) and decreased TGFβ signaling,[17] this suggested a potential mechanism for our previous observations that cholesterol-loading of mouse vascular smooth muscle cells (mVSMCs) promoted the down-regulation of contractile genes.[18,19]

That cholesterol-loading may lower TGFβ signaling also in VSMCs is reinforced by the findings that in loaded cells[19] and in the aortae of hypercholesterolemic mice,[20] *Mir143/145* are down-regulated. These microRNAs are positively regulated by TGFβ[21] and are known to promote the expression of messenger RNAs (mRNAs) associated with the contractile state.[22] Interestingly, *Mir143/145* suppresses KLF4, a monocyte differentiation factor.[22,23] When KLF4 was knocked out in hypercholesterolemic mice, the percentage of cells of VSMC origin that expressed macrophage markers was reduced by 50%.[24] Thus, it is possible that loss of TGFβ signaling on cholesterol-loading can account for both the loss of the contractile state and the acquisition of macrophage characteristics.

If the mechanism for the suppressive effects of cholesterol-loading on TGFβ signaling in VSMCs is similar to that discovered in epithelial and endothelial cells, namely the partitioning of its receptors to lipid rafts,[17] this may also provide insight into the dynamic regulation of VSMC phenotypic transitions to macrophage-like cells. Our previous study has shown that high-density lipoprotein (HDL)-promoted cholesterol efflux reverses the effects of cholesterol-loading on mVSMCs in vitro.[19] Notably, HDL reduces lipid rafts in monocytes and macrophages by depleting them of cholesterol.[25,26] Taken together, this suggests that the reversal of the cholesterol-loaded VSMC phenotype by HDL may be through its restoration of TGFβ signaling after displacement of its receptors from lipid rafts. That this may contribute to atheroprotection would be consistent with the clinical data that functional (ie, efflux-competent) HDL particles are associated with decreased cardiovascular disease event rates (eg, see Khera et al[27] and Rohatgi et al[28]) and the preclinical data that raising HDL particle levels promotes plaque regression and increases fibrous cap formation.[29-31]

In the present study, therefore, we aimed at defining the relationships among HDL, cholesterol-loading, TGFβ signaling, *Mir143/145* expression, and VSMC phenotypes. We have extended our previous studies in mVSMCs to human vascular smooth muscle cells (hVSMCs) of the coronary artery. We have also studied genetically altered atherosclerotic mice with reduced expression of *Tgfβr2*. As will be presented, cholesterol-loading of hVSMCs indeed partitions the receptors into lipid rafts and impairs TGFβ signaling and *Mir143/145* expression. Furthermore, phenotypic switching of cholesterol-loaded hVSMCs to a noncontractile, macrophage-like state was reversed by increasing the levels of functional HDL particles, which displaced TGFβ receptors from lipid rafts and restored signaling. The mouse data we will present also indicate that the loss of the VSMC contractile phenotype in vivo may be restored when the level of functional HDL particles is raised. Taken together, our findings present TGFβ signaling as a key regulatory pathway of VSMC plasticity in hypercholesterolemic settings, with the potential to provide atheroprotection by the restoration of the signaling in intimal cells of VSMC origin.

METHODS

CELL CULTURE. Human coronary artery smooth muscle cells (referred to as hVSMC) were purchased from Cell Applications and maintained in complete medium (#311-500) as provided by the vendor. hVSMCs were used within 8 passages for all experiments. Cells were cultured until 90% confluence in 37 °C in a 5% CO_2 incubator. For cholesterol or TGFβ1 treatment, cells were serum starved for 24 hours in 0.2% bovine serum albumin (BSA) (in basal media without serum; #310-500, Cell Applications), and treatments including methyl-β-cyclodextrin-cholesterol mixture (5 μg/mL, Sigma; hereafter referred to as cholesterol treatment), methyl-β-cyclodextrin (20 mmol/L; Sigma) TGFβR1 inhibitor (SB431542, Sigma), and recombinant human TGFβ1 (R&D Systems) were performed.

CHOLESTEROL-LOADING. Cholesterol was delivered to cells by using Chol:MβCD complex obtained from Sigma (C4951) containing approximately 50 mg of cholesterol/g solid (molar ratio, 1:6 cholesterol/MβCD). For all experimental conditions, treatment concentrations involving Chol:MβCD were based on cholesterol weight.

CHOLERA TOXIN STAINING. hVSMCs were grown in 8-chamber slides. After treatment, cells were washed with phosphate-buffered saline (PBS) twice, and lipid rafts were stained with cholera toxin B (CTB) using Vybrant Alexa Fluor 488 Lipid Raft Labeling Kit (#V-34403; Molecular Probes, Thermo Fisher Scientific) as per manufacturer instructions. Briefly, cells were

labelled with Alexa-fluor 488 CTB for 10 minutes at 4 °C, washed 4 times with chilled PBS. To crosslink CTB, cells were incubated with anti-CTB antibody for 15 minutes at 4 °C, washed 4 times with chilled PBS, and then fixed with 4% formaldehyde for 15 minutes at 4 °C. After washing 4 times with chilled PBS, cells were permeabilized with 0.1% Triton X-100 at room temperature and stained with Alexa Fluor 647 Anti-Smad2 phospho-SMAD2/3 (#ab311069; 1:50; Abcam) overnight at 4 °C. Nuclei were stained with 4',6-diamidino-2-phenylindole (DAPI) and slides were mounted with prolong antifade mounting medium (P-7481; Thermo Fisher Scientific) and then visualized by confocal microscopy.

HUMAN HDL ISOLATION AND APOA1 PURIFICATION. Human plasma was obtained from New York University Langone Medical Center blood bank. HDL was isolated from plasma by a sequential flotation ultracentrifugation method. Briefly, 30 mL of plasma was overlayed with 20 mL of 1.019 g/mL KBr density solution in 70-mL polycarbonate centrifuge tubes and ultracentrifuged at 40,000 revolutions/min for 24 hours at 4 °C to separate chylomicrons, intermediate-density lipoprotein, and very low-density lipoprotein as upper fractions. The lower fraction containing low-density lipoprotein and HDL was collected, adjusted to 1.080-g/mL density with KBr and overlaid with 1.063-g/mL KBr density solution and ultracentrifuged at 40,000 revolutions/min for 24 hours at 4 °C. The upper fraction (containing low-density lipoprotein) was removed, and the lower fraction (containing HDL and plasma proteins) was collected. Samples were adjusted to 1.225-g/mL density with KBr and overlaid with 1.21 g/mL of KBr solution and ultracentrifuged at 40,000 revolutions/min for 24 hours at 4 °C. The upper fraction containing HDL was collected and stored at −80 °C until APOA1 purification, as described in Wilhelm et al.[32]

MICE. All experimental procedures were done in accordance with the New York University Grossman School of Medicine's Institutional Animal Care and Use Committee (approved protocol #IA16-00519). ROSA26$^{mT/mG}$. Myh11-CreERT2/J mice and ROSA26$^{mT/mG}$. Myh11-CreERT2; Tgfβr2$^{fl/fl}$/J mice containing Myh11-CreERT2 inserted on the Y chromosome[33] were obtained from Dr George Tellides (Yale School of Medicine). For animal studies, all analyses were blinded whenever possible through numerical coding of samples. All mouse lines were in the C57BL/6J background.

Male mice of 8 weeks of age were intraperitoneally injected once with the mPCSK9D377Y gain-of-function transgene at 1.1 × 10^{12} viral particles/mouse (Penn Vector Core, University of Pennsylvania). Two weeks post-PCSK9 injection, Cre-lox recombination was induced by injecting tamoxifen (Sigma) intraperitoneally at 1 mg/dose for 5 days. Mice were then placed on Western diet (containing 21% fat, 0.3% cholesterol; Diets Inc) for 20 weeks, ad libitum to develop advanced atherosclerotic plaques. Mice were monitored regularly and mice with a total cholesterol level <400 mg/dL were excluded from the study.

ApoA1/HDL-MEDIATED ATHEROSCLEROSIS REGRESSION. Mice were randomly assigned to either progression (saline injection) or regression (ApoA1 injection) groups. To promote plaque regression, mice were continued on Western diet and ApoA1 (500 μg/mice) was administered subcutaneously twice a week for 2 weeks (weeks 21-23). Previous studies have shown that injected ApoA1 rapidly associates with HDL particles.[34] Saline injections served as vehicle control.

PLAQUE MORPHOMETRICS AND IMMUNOHISTOCHEMISTRY. In vivo samples. Aortic root sections were fixed with 4% paraformaldehyde for 15 minutes, permeabilized with 0.1% Triton X-100 for 30 minutes, followed by blocking with 3% BSA in PBS. Sections were stained with CD68 (Bio-Rad) overnight at 4 °C. Sections were then incubated with Alexa-Fluor 647 goat anti-rat IgG secondary antibody (Life Technologies) and stained with DAPI to detect nuclei. Images were acquired on Leica TCS SP5 confocal microscope. For some samples, sections were stained with Phospho-SMAD2 (Ser465, Ser467) Polyclonal Antibody (Thermo Fisher Scientific) followed by staining with FITC Anti-GFP antibody (Abcam), and DAPI staining to detect nuclei. Image processing and quantification of the stained area were performed using Image-Pro Plus software (Media Cybernetics).

In vitro samples. hVSMCs were grown on sterile glass coverslips. After serum starvation (0.2% BSA in complete media) for 24 hours, cells were treated for 24 hours. Cells were washed with PBS twice and then fixed in 4% paraformaldehyde for 10 minutes. After being rinsed with PBS twice, cells were permeabilized with 0.1% TritonX-100 for 5 minutes, followed by blocking in 4% normal goat serum in PBS. Anti-SMAD2/3 antibodies (Cell Signaling) were incubated at 1:200 dilution at 4 °C overnight. Alexa-Flour 488-conjugated goat anti-rabbit IgG (Life Technologies) was used to detect SMAD2/3 localization. Then, Alexa-Flour 568- Phalloidin (Life Technologies) was incubated at 1:50 dilution for 30 minutes. Coverslips were put on slides and mounted with medium containing DAPI. Images were acquired using Leica TCS SP5 confocal microscopy.

AORTIC DIGESTION AND FLOW CYTOMETRY. Mouse aortic arches were incubated in digestion buffer containing liberase (#273582, Roche), hyaluronidase (#3506, Sigma), DNase I (#DN25, Sigma), and 1 mol/L $CaCl_2$ at 37 °C for 15 minutes using the GentleMacs dissociator (Miltenyi Biotech). The digested tissue was passed through a 70-μm cell strainer, washed with 1× cold PBS and centrifuged at 350*g* for 10 minutes at 4 °C. Cells were incubated with viability dye eFluor 780 (eBioscience) for 30 minutes on ice, blocked with TruStain fcX (BioLegend), and then stained with PE/Cy7 anti-mouse CD11b antibody (#101216; BioLegend) and BV605 anti-mouse F4/80 (#123133; BioLegend) for 30 minutes on ice. Following this, SMCs lineage-positive (GFP^+) cells that were double positive for CD11b and F4/80 macrophage markers were sorted on a FACSAria II cytometer (BD Biosciences) equipped with a 100-μm nozzle, and were stored in TRIzol reagent (Invitrogen) for RNA isolation.

REAL-TIME qPCR. Total RNA was isolated from cultured hVSMCs using TRIzol reagent. Complement DNA was synthesized from total RNA using Verso cDNA Synthesis Kit (Thermo Fisher Scientific) or TaqMan MicroRNA Reverse Transcription Kit (Applied Biosystems) according to the manufacturer's instructions. For real-time quantitative polymerase change reaction (qPCR), specific mRNA or *MiR143/145* was amplified using Power SYBR Green PCR Master Mix (Applied Biosystems) or TaqMan Universal PCR Master Mix, No AmpErase UNG (Applied Biosystems), respectively. Expression was normalized to *GAPDH* for mRNAs or *U6* for miRNAs.

hVSMCs EVs. A total of 2×10^6 hVSMCs were seeded in to tissue culture flasks and incubated with 15 mL of serum-free complete medium (#311-500) for 24 hours under control or cholesterol-treated (methyl-β-cyclodextrin-cholesterol mixture 5 μg/mL [Sigma]) conditions using an established protocol.[35,36] Extracellular vesicles (EVs) were isolated from conditioned cell culture media using differential ultracentrifugation. Cell culture supernatants were harvested and cleared of cellular debris by centrifugation at 1,000*g* for 10 minutes at 4 °C. Cleared supernatants were transferred to new 15-mL tubes and stored at −80 °C until processed. Samples were thawed on ice and centrifuged at 1,000*g* for 10 minutes at 4 °C. Supernatants were transferred to 13.2-mL QuickSeal tubes (Beckman Coulter) and were centrifuged at 120,000*g* for 120 minutes at 4 °C with a MLA55 fixed-angle rotor using an Optima MAX-XP ultracentrifuge (Beckman Coulter). The pelleted hVSMC-derived EVs were resuspended in 100 μL of PBS and washed in 13.2 mL of PBS by ultracentrifugation at 120,000*g* for 60 minutes at 4 °C. Subsequently, pelleted hVSMC-derived EVs were resuspended in 100 μL of PBS (Thermo Fisher Scientific) for subsequent analysis.

NANOPARTICLE TRACKING ANALYSIS. hVSMC-derived EV particle size distribution and concentration profiles were determined by nanoparticle tracking analysis using a Zetaview device (Particle Metrix) as previously described (Akbar et al).[36] The Zetaview measured the sample chamber from 11 different positions in 2 continuous cycles. The settings were set at sensitivity 80, frame 30, and shutter speed 100. Silica 100-nm microspheres (Polysciences Inc) were used to quality check the instrument performance daily. Prior to injection into the sample chamber, samples were diluted in PBS 1:1,000.

WESTERN BLOTTING. Cells were washed with PBS twice, and protein was extracted in radioimmunoprecipitation assay buffer containing protease inhibitor mixture (Sigma) and phosphatase inhibitor cocktail (Roche). Protein concentration was determined by Bradford method (Bio-Rad). Equal amounts of protein were fractionated by sodium dodecyl sulfate-polyacrylamide gel electrophoresis, transferred to nitrocellulose membranes (Whatman). The membrane was blocked with 5% nonfat milk or 5% BSA for 1 hour, and then incubated with the indicated primary antibody overnight at 4 °C. After a 1-hour incubation with the appropriate secondary antibody, specific signals were detected by ECL chemiluminescent detection reagent (GE Healthcare). The signals were quantified by densitometry analysis (Image J, National Institutes of Health). The primary antibodies used were as follows: ACTA2 (#A2547, Sigma); CNN1 (#M3556, DAKO); SRF (#5147, Cell Signaling); p38MAPK (#sc-535, Santa Cruz Biotechnology); SMAD2/3 (#8685, Cell Signaling); TUBA (#T-5168, Sigma); and SMAD2 (#3103, Cell Signaling), phospho-SMAD2 (#3101S, Cell Signaling), phospho-p38MAPK (#9211S, Cell Signaling), SMAD4 (#9515, Cell Signaling); CD68 (#MCA1815, AbD Serotec, Bio-Rad); KLF4 (#12173, Cell Signaling); PU.1 (#sc-352, Santa Cruz Biotechnology); TGFβR1 (#3712, Cell Signaling); TGFβR2 (#sc-400, Santa Cruz Biotechnology); Caveolin (#610059, BD Transduction Laboratories); CD71 (#13113, Cell Signaling); GAPDH (#AM4300, Ambion).

IMAGING AND ANALYSIS. Images were acquired Leica TCS SP5 confocal microscope. Image processing, analysis, and cell counting were performed using Image J software.

siRNA AND microRNA MIMIC/INHIBITOR TRANSFECTIONS. *Mir143/145* mimics (60 nmol/L)/inhibitors (60 nmol/L) and small, interfering RNA (siRNA)

(60 nmol/L) against human KLF4 (On-Target plus SMART pool siRNA) were purchased from Dharmacon. hVSMCs were transfected with 60 nmol/L of siRNA or microRNA mimic/inhibitor using RNAiMAX transfection reagent (Invitrogen) according to the manufacturer's instructions. At 24 hours post transfection, treatments were performed as indicated elsewhere.

CELLULAR CHOLESTEROL MEASUREMENT. Cellular lipids were extracted by using a hexane/isopropyl alcohol (3:2) mixture, followed by cellular protein extraction with 0.2 N NaOH as described.[37] Total cholesterol was determined by using kits from Wako. Total cellular protein content was determined using Bradford assay (Bio-Rad).

TGFβ ASSAY. The TGFβ concentration was measured using mink lung epithelial cells stably transfected with an expression construct containing a truncated plasminogen activator inhibitor-1 promoter fused to the firefly luciferase reporter gene as described.[38] The cells were kindly provided by Drs D. Rifkin and J. Munger (New York University Grossman School of Medicine).

LIPID RAFT ISOLATION. Lipid rafts were fractionated as described,[39] followed by Western blotting. All steps were performed on ice. Briefly, cells were washed and then scraped in base buffer (20 mmol/L Tris-HCl, pH 7.8, 250 mmol/L sucrose, supplemented with 1 mmol/L $CaCl_2$ and 1 mmol/L $MgCl_2$). Cells were subjected to centrifugation for 2 minutes at 250*g* and the resulting pellet was resuspended in 1 mL of base buffer containing protease inhibitors. Cells were lysed by passage through a 22-G × 3-inch needle 20×, and the lysates were centrifuged at 1,000*g* for 10 minutes. The resulting post nuclear supernatant was collected and transferred to a separate tube. Then 1 mL of base buffer (+ protease inhibitor) was added to the cell pellet and passed through the needle and syringe 20× for lysis. The resulting lysate was centrifuged at 1,000*g* for 10 minutes, and the second post nuclear supernatant was combined with the first. An equal volume (2 mL) of 50% OptiPrep (diluted in base buffer) was added to the combined post nuclear supernatants and placed in the bottom of a 12-mL centrifuge tube. An 8-mL gradient of 0%-20% OptiPrep in base buffer was layered on top of the lysate, which was now 25% OptiPrep. Gradients were centrifuged for 90 minutes at 52,000*g* using an SW-41 rotor in a Beckman ultracentrifuge. A distinct band was observed at the interface between the 20% end of the gradient and the 25% OptiPrep bottom layer. Gradients were collected into 0.67-mL fractions, and the distribution of various proteins was assessed by Western blotting.

STATISTICS. All statistical analyses were performed using Prism 9 (GraphPad, Dotmatics). A Shapiro-Wilk test indicated that the data were normally distributed, $W = 0.95$, $P = 0.28$. P values were calculated using an unpaired Student's t-test for pairwise data comparisons or 1-way analysis of variance for data comparisons of 2 or more independent groups followed by Dunnett or Šídák post hoc test for comparison. A P value of ≤0.05 was considered significant.

RESULTS

CHOLESTEROL-LOADING OF hVSMCs LEADS TO DOWN-REGULATION OF CONTRACTILE GENE EXPRESSION. Previously we demonstrated that cholesterol-loading in mVSMCs down-regulated contractile gene expression.[18,19] To extend the observations to hVSMCs, we used human coronary artery VSMCs as a model system. Cholesterol-cyclodextrin complex was used to deliver cholesterol to hVSMCs as previously described.[19,40] Increases in the cellular contents of total cholesterol (Supplemental Figure 1A), neutral lipid (presumably cholesteryl ester) and decrease in α-smooth muscle actin (α-SMA) (Supplemental Figure 1B) confirmed the effectiveness of the loading protocol. MTT, 3-(4,5-dimethylthiazol-2-yl)-2,5-diphenyltetrazolium bromide, assays were performed to assess cell viability, which showed no adverse effects of cholesterol loading for at least 60 hours (Supplemental Figure 1C).

Consistent with our studies in mVSMCs, there was a time-dependent decrease in the expression of the contractile gene SMC marker *Acta2*, by ∼50% after 24 hours and ∼75% after 48 hours of cholesterol-loading (**Figure 1A**). We also determined the expression for other VSMC contractile-state markers, namely *Tagln* and *Cnn1*, and these were also down-regulated (**Figure 1B**). We have reported that in mVSMCs, cholesterol-loading down-regulated the expression of 2 key transcription factors, *Myocd* and *Srf*, which govern the contractile VSMC phenotype.[19] Indeed, *Myocd* and *Srf* mRNAs were also down-regulated in cholesterol-loaded hVSMCs (**Figure 1B**). We also confirmed the down-regulation of α-SMA and CNN1 at the protein level (**Figures 1C to 1E**).

Taken together, our data indicate that cholesterol-loading down-regulates the expression of contractile-state-associated genes in hVSMCs in vitro.

TGFβ SIGNALING IS DOWN-REGULATED IN CHOLESTEROL-LOADED hVSMCs. Having established an attenuated hVSMC contractile phenotype with cholesterol-loading, we next wanted to

FIGURE 1 **Contractile Gene Expression Is Downregulated in Chol-Loaded hVSMCs**

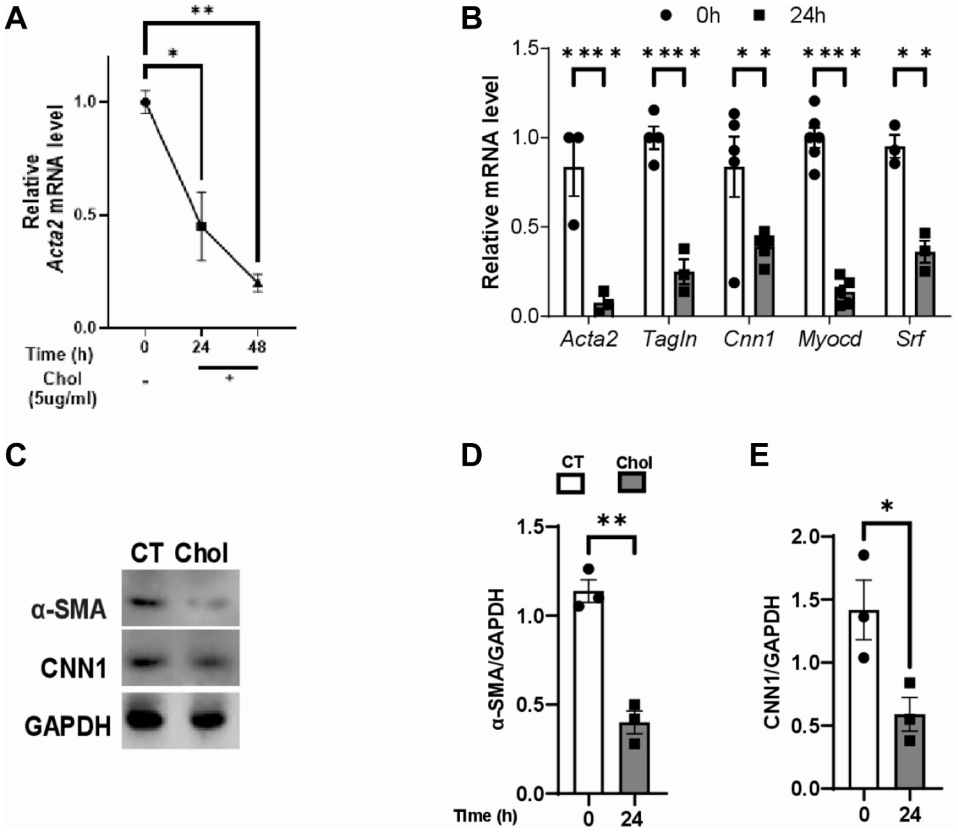

(A, B) Human vascular smooth muscle cells (hVSMCs) were treated with cholesterol (Chol) (5 μg/mL) or 0.2% bovine serum albumin (control [CT]) for 24 hours and 48 hours and gene expression of *Acta2*, *Tagln*, *Cnn1*, *Myocd*, and *Srf* were determined by quantitative polymerase chain reaction. (C) hVSMCs were treated with Chol (5 μg/mL) or 0.2% bovine serum albumin (CT) for 24 hours and protein expression of α-smooth muscle actin (α-SMA) and CNN1 were determined by Western blotting (representative blots shown). Densitometry showing the (D) α-SMA and (E) CNN1 band intensities normalized to GAPDH. For data analysis, unpaired Student's *t*-testing was performed for comparing the means of 2 groups. For 2 or more independent groups, 1-way analysis of variance followed by Dunnett post hoc test was performed. A *P* value of ≤0.05 was considered significant. Data are presented as the mean ± SEM of 3 independent experiments, and *P* values are as indicated (*$P < 0.05$, **$P < 0.01$, ****$P < 0.0001$).

understand the mechanism for this. We focused on the TGFβ pathway because of its prominence in promoting the contractile state of VSMCs across species[13] and a pilot study that suggested cholesterol-loading reduces TGFβ signaling in mVSMCs.[19]

Additionally, we were interested in the connections among TGFβ signaling, Mir143/145, and cholesterol-loading based on multiple lines of reasoning. 1) TGFβ signaling positively regulates hVSMC contractile phenotype in part by promoting the expression of Mir143/145.[22] 2) Cholesterol-loading in mVSMCs down-regulates *Mir143/145*, resulting in the loss of the contractile phenotype, and *Mir143/145* mimics protect against this loss.[19] 3) Consistent with this, *Mir143/145* expression is down-regulated in aortic VSMCs in hypercholesterolemic *ApoE*$^{-/-}$ mice,[20,41] and in epithelial and endothelial cells cholesterol loading attenuates TGFβ signaling.[17,42] Then the following series of experiments were performed to test the model that cholesterol-loading reduces TGFβ signaling, which in turn decreases Mir143/145 expression, resulting in the diminution of the contractile phenotype of hVSMCs.

As shown in **Figures 2A and 2B**, hVSMCs treated with TGFβ1 exhibited up-regulation of the transcripts of the precursors of Mir143 and Mir145, namely pri-Mir143 and pri-Mir145; strikingly, in the cholesterol-loaded cells, the responses to TGFβ1 treatment were attenuated. Furthermore, the expressions of contractile genes *Acta2* and *Tagln* were induced by TGFβ1 in control hVSMCs, but this was also attenuated in cholesterol-loaded cells (**Figures 2C and 2D**).

FIGURE 2 **Chol-Loading Downregulates TGFβ Signaling in hVSMC**

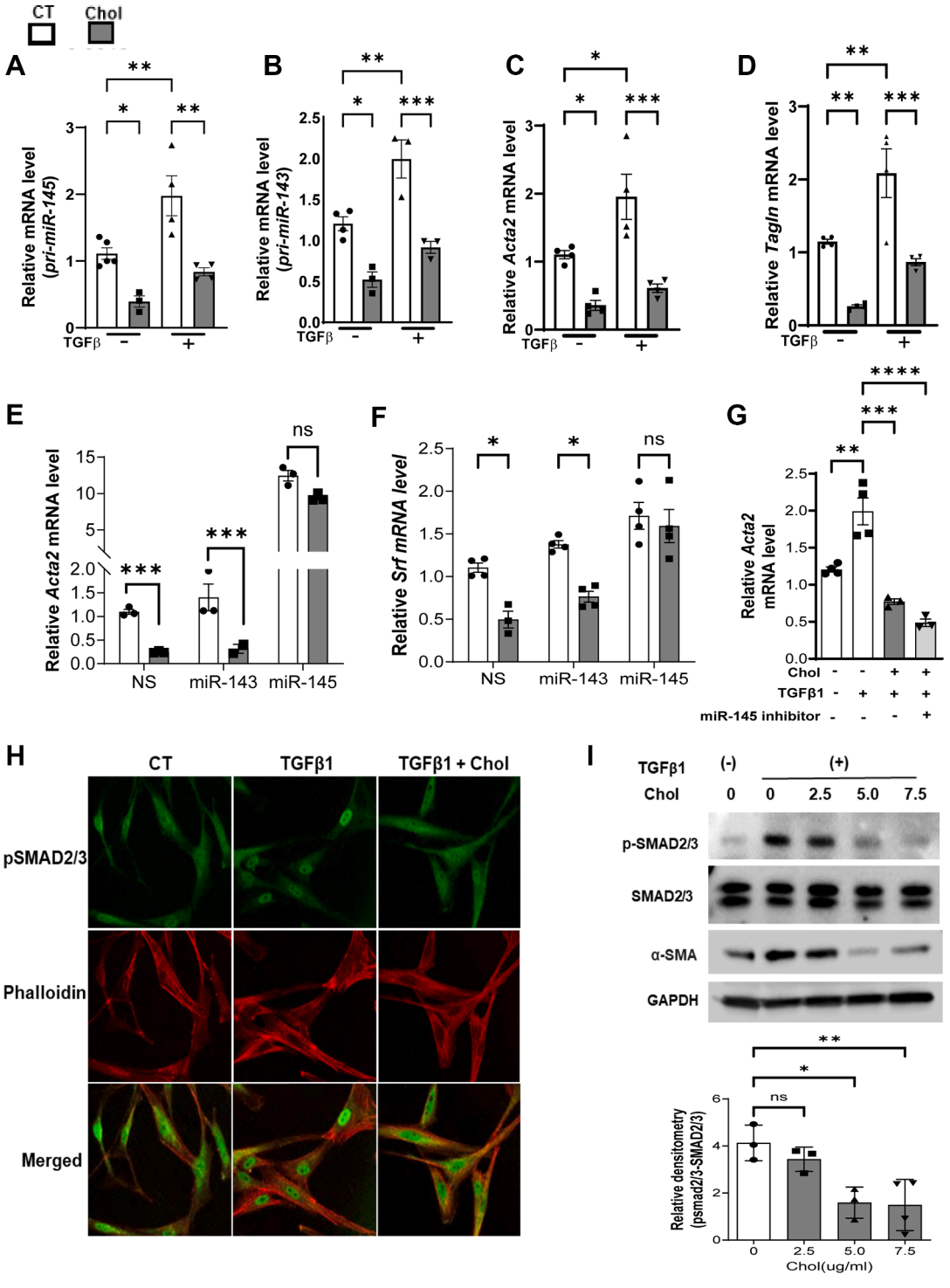

Continued on the next page

Next, we overexpressed Mir143 or Mir145 mimics in control or in cholesterol-loaded hVSMCs. Of the 2 mimics, only Mir145 up-regulated the level of *Acta2* mRNA in cholesterol-loaded hVSMCs to a comparable level to that in unloaded cells (**Figure 2E**). In addition, the Mir145 mimic prevented the suppression of *Srf,* a master regulator of the VSMC contractile phenotype in cholesterol-loaded cells (**Figure 2F**). Henceforth, we focused on Mir145 for further studies. As shown in **Figure 2G**, the level of *Acta2* mRNA in TGFβ1-treated cholesterol-loaded cells was attenuated compared to that in TGFβ1-treated nonloaded cells. Notably, in the presence of a Mir145 inhibitor, in cholesterol-loaded VSMCs TGFβ1 treatment failed to increase *Acta2* mRNA over that in the control cells. These results suggest that the efficacy of TGFβ1 to oppose the effects of cholesterol-loading on contractile gene expression depends on its ability to induce Mir145 (**Figure 2G**).

To extend these findings, we next directly determined whether cholesterol-loading decreased TGFβ1 signaling. Despite no changes in the expression levels of key downstream factors total SMAD2/3 by either cholesterol-loading (Supplemental Figure 2A) or TGFβ1-signaling inhibition using SB431542[43] (Supplemental Figure 2B); both of these treatments decreased contractile gene expression (*Acta2*) in hVSMCs (Supplemental Figure 2C and **Figure 1**, respectively), and by confocal microscopy, cholesterol decreased the level of active (nuclear) SMAD phosphorylated species even in the presence of TGFβ (**Figure 2H**). In an independent analysis (**Figure 2I**), the cholesterol-loading-associated decrease in TGFβ1 stimulation of SMAD2/3 phosphorylation was dose-dependent and resulted in reduced expression of α-SMA at the protein level.

In these experiments, exogenous TGFβ1 was added. VSMCs are known to secrete TGFβ1. To see whether there is the potential for an autocrine/paracrine pathway based on endogenous production in the in vitro model, we measured the concentrations of both the active and latent forms of TGFβ1 in the conditioned medium of hVSMCs. As shown in Supplemental Figure 3, the level of the active form (~30 pg/mL) (Supplemental Figure 3A) was sufficient to activate signaling in a reporter cell assay (Supplemental Figure 3B) and was in the range of the concentration of recombinant TGFβ1 that promotes SMAD2/3 phosphorylation and α-SMA induction (Supplemental Figure 3C).

Overall, the results in this section support the model proposed herein, namely that cholesterol-loading reduces TGFβ signaling, which in turn decreases Mir143/145 expression, resulting in the attenuation of the contractile phenotype in hVSMCs. Furthermore, the pool of TGFβ1 whose signaling is being regulated by cholesterol-loading may be a component of an autocrine/paracrine process.

CHOLESTEROL-LOADING PARTITIONS TGFβR1/R2 TO LIPID RAFTS AND IS ASSOCIATED WITH LOSS OF TGFβ SIGNALING. Lipid rafts are small free cholesterol-enriched portions of plasma membranes. The signaling activity of receptors can vary depending on their presence or absence in lipid rafts.[44] It has been reported that free cholesterol-loading increases lipid raft domains in multiple cell types, including VSMCs.[45] Previous studies alluded to herein in (mink lung) epithelial cells and (bovine aortic) endothelial cells have shown that when the receptor complex for TGFβ1, TGFβR1/R2 heterodimers, are in lipid rafts, TGFβ signaling is suppressed.[17,46-49] Given the results in the previous section, implicating cholesterol enrichment of hVSMCs with loss of TGFβ signaling, we hypothesized that this was because of consequent enrichment in lipid raft partitioning of TGFβ receptors.

To test this hypothesis, we determined the effects of cholesterol-loading on the distribution of TGFβR1/R2 in plasma membranes of hVSMCs. As shown in **Figure 3**, cholesterol-loading resulted in enrichment of the receptor complex in the lipid raft region

FIGURE 2 Continued

hVSMCs were treated with Chol (5 μg/mL) or 0.2% bovine serum albumin (CT; ie, 0 μg/mL cholesterol) for 24 hours in the presence or absence of TGFβ1 ligand (10 pg/mL). Total RNA was isolated and quantitative polymerase chain reaction (qPCR) was performed to determine the *pri-Mir143/145* precursor transcripts (A,B) or SMC markers, *Acta2* and *Tagln* (C,D). hVSMCs were treated as in A and B, but either in the presence or absence of TGFβ1 10 pg/mL) and/or nonscrambled (NS) or *Mir145* mimic (60 nmol/L). qPCR was performed to determine expression of *Acta2* (E) and (F) *Srf* mRNA. (G) hVSMCs were treated as in A and B, but either in the presence or in absence of TGFβ1 (10 pg/mL) and/or *Mir145* inhibitor (60 nmol/L). qPCR was performed to determine expression of *Acta2.* (H) Immunofluorescence images of total SMAD2/3 (green) in hVSMCs after 24 hours of the indicated treatments. Cytoplasm was stained with phalloidin (red). Nuclei were determined as phalloidin negative area (bar = 50 μm). (I) hVSMCs were treated as in A and B, but with varying amounts of Chol and in the presence or absence of recombinant TGFβ1 (10 pg/mL) for 24 hours. Proteins were extracted for Western blotting to detect phosphorylated (p) SMAD2/3, and α-SMA. Total SMAD2/3 or GAPDH was used as loading CT proteins. Blots are representative of at least 3 independent experiments, and the replicates were quantified by densitometry. For data comparisons of 2 or more independent groups, 1-way or 2-way analysis of variance followed by Dunnett post hoc test was performed. Data are presented as the mean ± SEM of 3 independent experiments, and *P* values are as indicated (*$P < 0.05$, **$P < 0.01$, ***$P < 0.001$, ****$P < 0.0001$). ns = not significant; other abbreviations as in **Figure 1**.

FIGURE 3 Cholesterol-Loading Partitions TGFβ Receptors Into Membrane Lipid Rafts

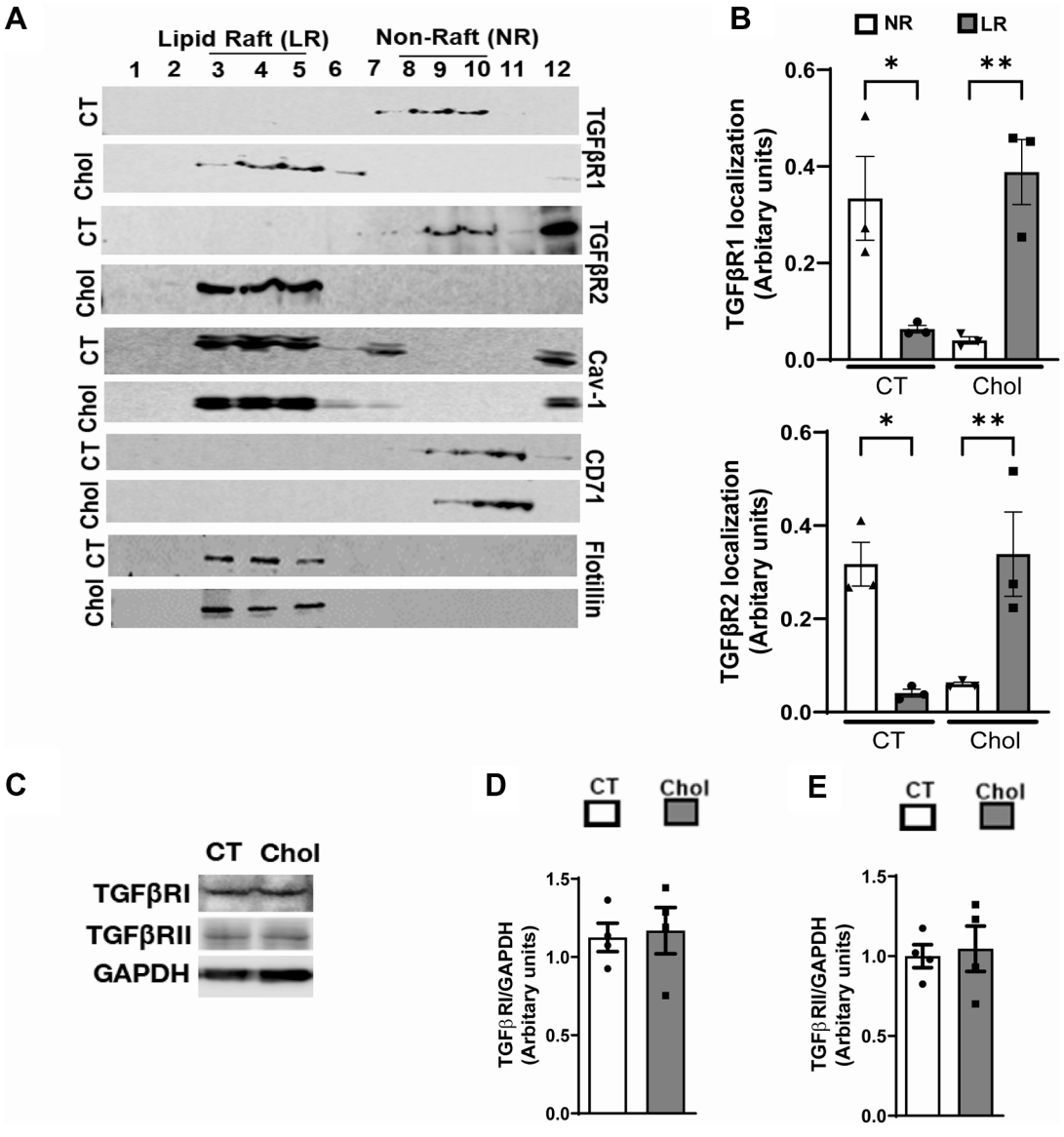

hVSMCs were treated with Chol (5 μg/mL) or 0.2% bovine serum albumin for 24 hours. (A) Membrane lipid raft (LR) and nonraft (NR) fractions were isolated, and Western blotting was performed using each of these fractions to determine the expressions of TGFβR1 and TGFβR2, as well as CAV1, flotillin, and transferrin receptor (CD71). (B) Densitometry was performed to quantify the levels of TGFβR1 and TGFβR2 in the LR and NR fractions. (C) Western blotting was performed from total cell lysates of Chol-treated or untreated cells, and the bands of the TGFβ receptors visualized. (D and E) Densitometry was performed to quantify the levels of TGFβR1 and TGFβR2. Blots are representative of 3 independent experiments. For data analysis, unpaired Student's *t*-test was performed for comparing the means of 2 groups. For 2 or more independent groups, 2-way analysis of variance followed by Dunnett post hoc test was performed. Data are presented as the mean ± SEM of at least 3 independent experiments, and *P* values are as indicated (*$P < 0.05$, **$P < 0.01$). Abbreviations as in Figure 1.

(gradient fractions 3-5), whereas in the control cells, the receptors were more abundant in the nonraft region (fractions 8-10) (**Figures 3A and 3B**). CAV1 and FLOT1 served as markers for lipid rafts. Transferrin receptor (CD71) served as a markers for nonraft fractions (**Figure 3A**).[39]

Because EV shedding can be greater from lipid rafts than from other plasma membrane domains,[50,51] another contributor to decreased TGFβ signaling could be the loss of the receptors themselves. Thus, we first determined the total EVs produced by cholesterol-loaded and unloaded hVSMCs. Indeed, cholesterol-loading increased the total number and concentration of EV-like particles released into the cell supernatants (Supplemental Figures 4A and 4B). Next, we isolated the EVs and performed enzyme-linked immunosorbent assay to determine the contents of TGFβR1/R2. There was no difference in the total recovery of either TGFβR1 or TGFβR2 in EVs from control or cholesterol-loaded hVSMCs (Supplemental Figures 4C and 4D). Consistent with this were the levels of TGFβR1 or TGFβR2 in whole cell lysates, which showed no differences in their expression between control and cholesterol-loaded hVSMCs (**Figures 3C to 3E**). This implies either those TGFβ receptors are associated with a subclass of EVs common to both conditions or that few TGF receptors are associated with EVs in general.

Overall, these results imply that it is the plasma membrane lipid raft distribution of the receptors, but not the receptor expression levels, that plays a key role in cholesterol-mediated dysregulation of TGFβ signaling.

HDL RESTORES THE SIGNALING OF TGFβ RECEPTORS AND REDISTRIBUTES THEM OUT OF LIPID RAFTS. We previously reported that HDL and ApoA1 (the HDL-forming apolipoprotein) reversed the reduction in mVSMC contractile gene expression.[19] Therefore, we wondered whether HDL restored contractile gene expression in cholesterol-loaded hVSMCs, and if so, whether it was by re-establishing TGFβ signaling by redistribution from lipid rafts. This would be consistent with the known ability of HDL to reorganize lipid rafts (ie, alter their distribution or lipid and protein composition) and modulate other signaling pathways.[26,52]

To begin to address this, we first assessed the role of HDL in regulating TGFβ signaling independent of cholesterol-loading. The data showed that hVSMC treatment with HDL had no significant increase in *Acta2* mRNA compared to TGFβ1 ligand treatment (Supplemental Figure 5A). To further explore whether HDL exhibits a cholesterol-loading independent role in hVSMCs, we performed cholera toxin staining to assess its effects on the level of lipid rafts. The data show that in the absence of cholesterol-loading, HDL has little effect on lipid rafts (Supplemental Figure 5B). Moreover, compared to control cells, HDL-treated cells showed similar levels of pSMAD2/3 levels (Supplemental Figure 5B).

Next, we loaded hVSMCs with cholesterol for 24 hours and then treated for 24 hours with HDL particles (isolated from human plasma; see the Methods section) to promote cholesterol efflux and lipid raft reorganization. As shown in **Figure 4A**, in hVSMCs that had been cholesterol-loaded, HDL restored SMAD2 phosphorylation in response to TGFβ1 to the level observed in nonloaded cells. Furthermore, the expressions of *Myocd,* Mir143/145 (**Figure 4B**), *Acta2* (**Figure 4C**), and *Cnn1* (**Figure 4D**) were also restored by HDL treatment in cholesterol-loaded cells. That this was related to HDL-mediated cholesterol efflux was supported by the increase in the expression of the sterol regulatory element binding protein-regulated gene *Hmgcr*, which was suppressed by cholesterol-loading (**Figure 4E**). To confirm that HDL mediated restoration of the contractile pattern of gene expression via TGFβ signaling, as suggested by the SMAD2 phosphorylation results, we employed SB431542, a TGFβR1 kinase inhibitor that decreases SMAD phosphorylation and TGFβ signaling.[43] As shown in **Figure 4F**, SB431542 (labeled as TGFβR1i) diminished the HDL-mediated effect on hVSMC α-SMA expression.

We next determined whether the restorations of TGFβ receptor signaling and contractile gene expression were related to HDL-induced lipid raft reorganization. As shown in **Figure 5A**, that HDL treatment was successful in reorganizing lipid rafts was indicated by CAV1 and FLOT1 now being found in the dense gradient fractions, which is consistent with studies showing that cellular cholesterol depletion relocalizes this protein from lipid rafts to Golgi/endoplasmic reticulum membranes,[53] which are found in the bottom fractions of the sucrose gradient. Concomitant with this redistribution of CAV1, both TGFβ receptors, which were previously enriched in lipid rafts after cholesterol-loading (**Figure 3**), were now predominantly in the non-lipid-rich fractions (**Figure 5A**; quantified from multiple gradients in **Figures 5B and 5C**), where they are more active in signaling.[17,46-49] Along with the redistribution of the lipid rafts, there was an increase in pSMAD2 levels (reflective of increased receptor signaling) in cholesterol-loaded hVSMCs incubated with HDL (**Figure 5D**).

Finally, to evaluate effects of HDL besides its ability to mediate cholesterol efflux, we used β-methyl cyclodextrin. Unlike HDL, β-methyl

FIGURE 4 HDL Treatment In Vitro Restores TGFβ Signaling in Cholesterol-Loaded hVSMCs

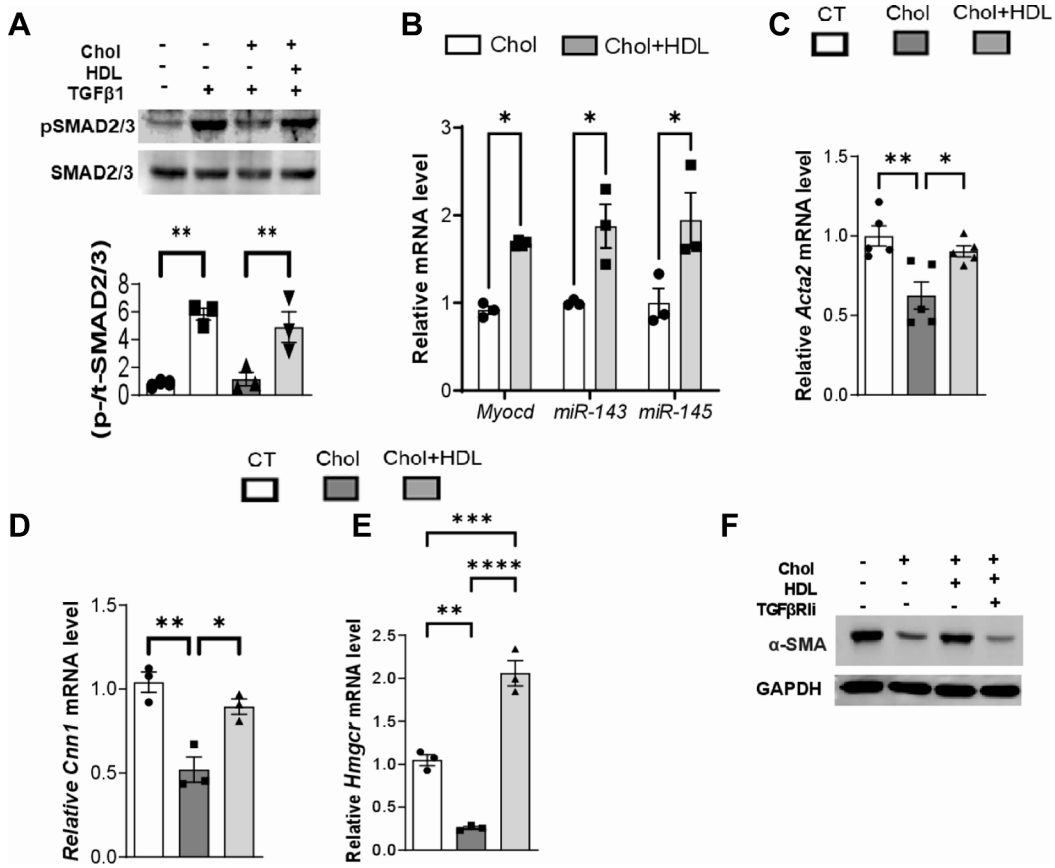

(A) hVSMCs were treated with Chol (5 μg/mL) or 0.2% bovine serum albumin for 24 hours, followed by high-density lipoprotein (HDL) (50 μg/mL) treatment for 48 hours. Then, treatment groups were stimulated with recombinant TGFβ1 (10 pg/mL). Western blotting was performed to detect pSMAD2 and total (t) SMAD2, with densitometry used for quantification. (B to E) qPCR was performed to detect expression of *Mir143/145*, *Myocd*, *Acta2*, *Cnn1*, and *Hmgcr* at the conclusion of the experiment in A. (F) Chol-loaded cells were either treated with HDL alone, HDL + TGFβR1 antagonist (TGFβR1i; 50 ng/mL), or left untreated. Western blotting was performed to detect α-SMA. GAPDH was used as loading CT protein. For data analysis of 2 or more independent groups, 1-way or 2-way analysis of variance followed by Dunnett post hoc test was performed. Blots are representative of 3-5 independent experiments (mean ± SEM). *P* values are as indicated (*$P < 0.05$, **$P < 0.01$, ***$P < 0.001$, ****$P < 0.0001$). Abbreviations as in Figures 1 and 2.

cyclodextrin primarily works by passive extraction of cholesterol from the plasma membrane without requiring, as does HDL, specific mechanisms (eg, ABCA1, ABCG1, SCARB1). As with HDL, we found that β-methyl cyclodextrin treatment of cholesterol-loaded hVSMCs increased *Acta2* mRNA levels, but the increase was not as high as with HDL (Supplemental Figure 5C). This may indicate that in addition to cholesterol efflux, other metabolic effects of HDL (such as reorganization of the actin cytoskeleton[26] or depletion of critical lipid raft proteins[54] may contribute to its restoration of a contractile phenotype in cholesterol-loaded VSMCs.

Using cholera toxin staining again as a marker for lipid rafts, cholesterol-loading, as expected, was shown to induce enrichment in lipid rafts (Supplemental Figure 5B), which correlated with reduced TGFβ signaling (as judged by pSMAD2/3 levels). Notably, β-methyl cyclodextrin and HDL treatment in cholesterol-loaded cells both increased pSMAD2/3 levels (Supplemental Figure 5B).

CHOLESTEROL-LOADING OF hVSMCs PROMOTES A MACROPHAGE-LIKE STATE, WHICH IS REVERSED BY HDL. We have previously reported in mVSMCs that cholesterol-loading resulted not only in the loss of the contractile phenotype, but the assumption of a macrophage-like state.[18,19] This was consistent with studies in mice and humans showing atherosclerotic plaques containing many macrophage-like cells (as

FIGURE 5 HDL Treatment Displaces TGFβ Receptor From Membrane Lipid Rafts in Chol-Loaded hVSMCs and Restores its Signaling

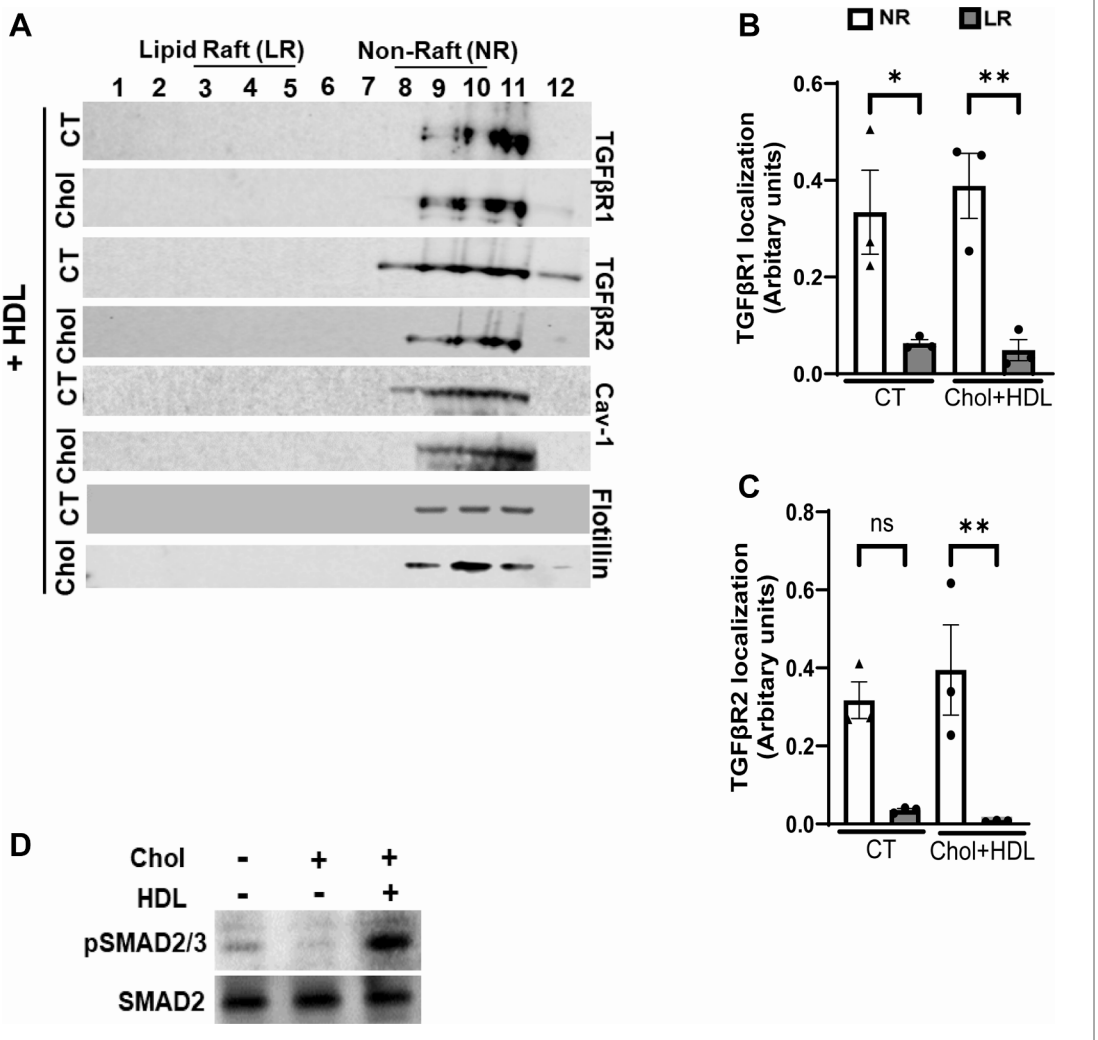

hVSMCs were treated with Chol (5 μg/mL) or 0.2% bovine serum albumin (CT) for 24 hours, after which they were all treated with HDL (50 μg/mL) for 24 hours. (A) At the end of the 48-hour protocol, LR and NR fractions were isolated, and Western blotting was performed using each of these fractions to determine the expressions of TGFβR1 and TGFβR2, as well as CAV1, and flotillin. Densitometry was performed to quantify the level of (B) TGFβR1 and (C) TGFβR2. (D) hVSMCs were loaded with Chol (48 hours, 5 μg/mL) and were then either treated with HDL (50 μg/mL) for 24 hours, or left untreated. Western blotting was performed to determine pSMAD2, SMAD2, and GAPDH levels. For data analysis of 2 or more independent groups, 2-way analysis of variance followed by Šídák multiple comparisons post hoc test was performed. Data are presented as the mean ± SEM of at least 3 independent experiments, and the *P* values are as indicated (*$P < 0.05$, **$P < 0.01$). Abbreviations as in Figures 1 to 4.

detected by marker expression) of VSMC origin (eg,[12,24,55-57]). Therefore, we sought to determine whether this could be explained by cholesterol-loading of hVSMCs and, if so, what the mechanism would be.

As shown in Figure 6A, at 48 hours, cholesterol-loading of hVSMCs again decreased the mRNA levels of *Acta2*, whereas that of *Cd68*, a commonly accepted macrophage marker, was up-regulated. Note that the time courses of these changes were different, with significant decreases in the mRNA levels for *Acta2* occurring at 24 hours and for *Cd68* at 48 hours. This temporal pattern suggested that the loss of TGFβ signaling (reflected by the decrease in *Acta2* mRNA expression) likely precedes the gain in the mRNA expression of the macrophage marker *Cd68*. We hypothesized that this represented a functional link between the loss of TGFβ signaling

and the gain of macrophage-like features. A prime candidate to be central in this link is KLF4, given that it is a known monocyte differentiation factor[58] whose expression is repressed by Mir143/145[22] (which, as was noted, are induced by TGFβ signaling),[21] and whose deficiency in mVSMCs reduced the macrophage-like cells in mouse atherosclerotic plaques by ∼36%.[24]

In an initial experiment, hVSMCs were cholesterol-loaded for 48 hours, which resulted in up-regulation of *Klf4* mRNA and protein (**Figures 6B and 6C**). Notably, the cholesterol-induced increase in CD68 was blocked by siRNA to *Klf4* (**Figure 6D**). We hypothesized that the effects of cholesterol-loading on *Klf4* expression were a result of the reduction in Mir143/145 as a consequence of decreased TGFβ signaling. This relationship was supported by the ability of a mimic of Mir145 to prevent the reduction in KLF4 and CD68 in cholesterol-loaded hVSMCs, while also increasing α-SMA (differences between treatments: CD68, $P = 0.024$; KLF4, $P = 0.018$; α-SMA, $P = 0.009$) (**Figure 6E**).

We next studied the effects of HDL on the phenotype of hVSMCs loaded with cholesterol. As shown in **Figure 6F**, KLF4 (**Figure 6F**) and CD68 expression (**Figure 6G**) were reduced by HDL. In addition, when an inhibitor of TGFβ signaling was used, the restorative effects of HDL were lost (**Figure 6H**).

Taken together, these results show that, as in mVSMCs, cholesterol-loading promotes macrophage-like features in hVSMCs and that HDL can reverse this and restore the contractile state. Furthermore, the likely mechanism involves the restoration by HDL of TGFβ signaling, which results in up-regulation of Mir143/145 and repression of KLF4.

HDL-MEDIATED REGRESSION REDUCES THE PERCENTAGE OF VSMC-DERIVED MACROPHAGE-LIKE CELLS IN THE ADVANCED ATHEROSCLEROTIC PLAQUE. Our results show that HDL mediates the transition of cholesterol-loaded hVSMC-derived macrophage-like cells back to a contractile VSMC phenotype by regulating TGFβ signaling in vitro. The current thinking is that macrophages and macrophage-like cells take up lipoproteins to form foam cells that contribute to plaque progression and inflammation.[3] There are currently no pharmacologic agents that are known to drive VSMC-derived macrophage-like foam cells toward their original phenotypic state, which are assumed to be atheroprotective. That this issue is relevant to both preclinical and clinical atherosclerosis is emphasized by the reports that at least one-half of the foam cells with macrophage features in human plaques are VSMC-derived,[55] with similar findings in mice.[56] Thus, based on our results in vitro, in which cholesterol-loading of hVSMCs promoted a macrophage-like phenotype and HDL reversed it, we hypothesized that a similar phenomenon could occur in vivo.

To test this hypothesis, we studied mVSMC lineage tracing mice (reported in Li et al[33]) with the partial conditional deletion of *Tgfβr2* (Myh11-CreERT2:ROSA26$^{mTmG/+}$: TgfβrII$^{fl/+}$; hereafter referred to as *Tgfβr2*$^{+/-}$ mice), and induced atherosclerosis via recombinant adeno-associated virus AAV.8 PCSK9 injection to raise cholesterol levels.[59] Mice with native TGFβ signaling (Myh11-CreERT2; ROSA26$^{mTmG/+}$; *Tgfβr2*$^{+/+}$), referred to as Tgfβr2$^{+/+}$ mice, were used as control animals. The use of partial knockdown of *Tgfβr2* in VSMCs allowed us to better determine whether HDL restored a VSMC contractile phenotype in hypercholesterolemic mice, because homozygous knockout mice manifest macrophage marker-positive cells of VSMC origin in the absence of hypercholesterolemia,[16] likely related to the total absence of VSMC TGFβ signaling.

After tamoxifen-induced recombination and AAV.8-PCSK9 injection, *Tgfβr2*$^{+/-}$- and *Tgfβr2*$^{+/+}$ mice were fed a Western diet for 16 weeks. One group of mice were injected with saline, which served as progression group, whereas another group was injected with ApoA1 (500 μg/dose/mice), which rapidly assembles into cholesterol-efflux promoting HDL particles.[32,34] We found no differences in body weights between the different groups and genotypes (Supplemental Figure 6A). In vivo efficacy of PCSK9 injection was confirmed by plasma total cholesterol (Supplemental Figure 6B). An increase in plasma HDL cholesterol was observed in ApoA1-injected mice, confirming the in vivo assembly of HDL from ApoA1 (Supplemental Figure 6C). Treatment was given every 2 days for 2 additional weeks of Western diet feeding (**Figure 7A**).

As expected, in the progression group, *Tgfβr2*$^{+/-}$ mice displayed a 20% increase in GFP$^+$ CD68$^+$ cells within the plaque compared to the *Tgfβr2*$^{+/+}$ mice, indicative of increased mVSMC assumption of a macrophage-like phenotype (**Figures 7B and 7C**). After the injections of ApoA1, the *Tgfβr2*$^{+/+}$ mice and *Tgfβr2*$^{+/-}$ mice exhibited 10% and 22% decreases (**Figure 7C**), respectively, in GFP$^+$ CD68$^+$ cells, suggesting that the macrophage-like phenotype of the plaque mVSMCs underwent at least partial reversion to the contractile phenotype. In an independent analysis, we found that SMCs (GFP$^+$ cells) expressed higher percent of macrophage markers

FIGURE 6 Macrophage Markers Upregulated in Chol-Loaded hVSMCs Are Suppressed by HDL Through Restoration of TGFβ Signaling

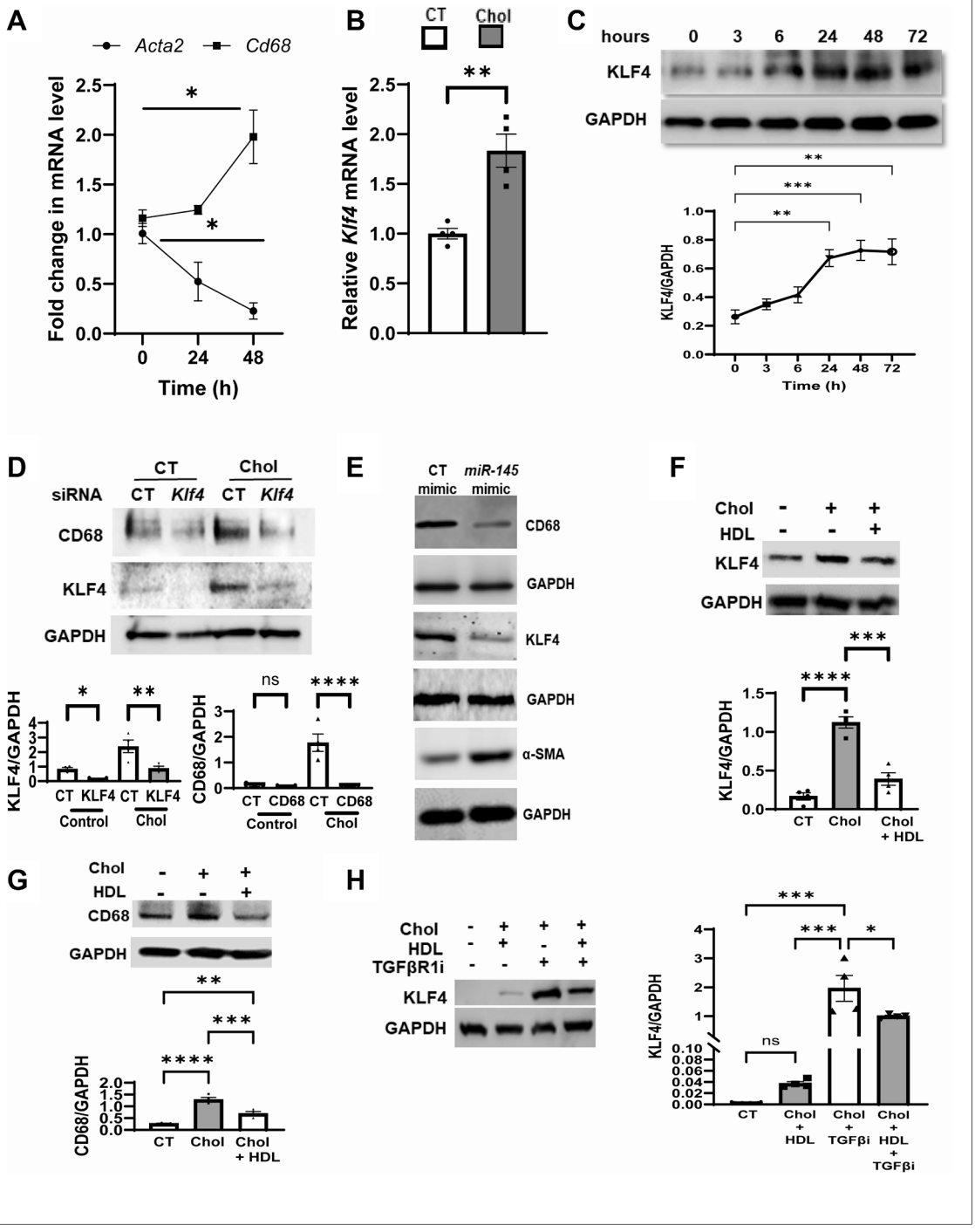

Continued on the next page

(GFP$^+$CD11b$^+$F4/80$^+$) in *Tgfβr2*$^{+/-}$ as compared to *Tgfβr2*$^{+/+}$ mice (Figure 7C). Conversely, in regressing mice, the percentage of GFP$^+$CD11b$^+$F4/80$^+$ cells was significantly reduced in *Tgfβr2*$^{+/+}$ compared to its corresponding progression group (Figure 7D). Similar changes in the percentage of GFP$^+$CD11b$^+$F4/80$^+$ cells were found in *Tgfβr2*$^{+/-}$ in regression as compared to their corresponding progression groups

(Figure 7D). Similarly, we found comparable increases in *Acta2* expression in both *Tgfβr2*$^{+/+}$ and *Tgfβr2*$^{+/-}$ in mice injected with ApoA1 (regression), compared to their respective progression groups (Figure 7E). To test that these changes were associated with increased TGFβ signaling, we also quantitated the number of cells immunopositive for pSMAD2. As shown in Figure 8, ApoA1 treatment was indeed associated with trends of increased positivity in both the wild-type mice and mice that are haplo-sufficient for *Tgfβr2* in plaques (Figure 8B) and in the media (Figure 8C).

DISCUSSION

VSMCs in normal arteries have been studied typically for their contractile functions. In atherosclerotic plaques, these cells migrate from medial layer into the intima and then proliferate,[10,60] where they can assume many fates. For example, these cells are major contributors to SMA^{+}, collagen-secreting cell population, thereby governing fibrous cap thickness and plaque stability.[61-63] Another fate in both mouse and human plaques is the acquisition of macrophage and macrophage foam cell-like features, either directly in vitro or after a transition in vivo to a multipotent SEM ("stem, endothelial, and monocyte") cell (reviewed in Miano et al[60]). Cells of VSMC origin are estimated to be a significant proportion (as high as ∼60%-70%) of the macrophage marker+ cell population in plaques.[56] Whereas the functional consequence of this is still a topic of speculation, the sheer abundance of these cells has called attention to the process whereby they originate, whether the process is reversible, and whether they contribute to the risk of adverse clinical events.

The present study provides insights into the mechanisms of hVSMC loss of the contractile phenotype and the transition to the macrophage-like phenotype in atherosclerotic plaques. First, we show that cholesterol-loading of hVSMCs dampens contractile and enhances macrophage gene expression in a time-dependent manner by impairing TGFβ signaling. Furthermore, an important consequence of this impairment is the decrease in the expression of Mir143/145, important molecular factors for the positive maintenance of the VSMC contractile phenotype and suppression of the macrophage-like features. The suppression of TGFβ signaling by cholesterol-loading was driven by TGFβR1/2 enrichment in lipid rafts. This result is supported by evidence that epithelial and endothelial cells that are cholesterol-loaded also undergo TGFβR localization to rafts and suppression of TGFβ signaling (reviewed in Chen et al[17]). It should be noted that another "negative feedback" regulator of TGFβ signaling in VSMCs has recently been described,[64] in which the protein LMO7, initially induced by TGFβ after vascular injury, subsequently reduces TGFβ transcription. Thus, depending on the context, vascular injury or hypercholesterolemia, these and other mechanisms to reduce TGFβ signaling may be operative.[65]

For example, we note a recent report[66] that showed that a direct interaction of the cytoplasmic tail of TGFβ receptor with the lipid raft marker Cav1 inhibited TGFβ1-stimulated signaling. Furthermore, β-methyl cyclodextrin-mediated cholesterol efflux to disrupt lipid rafts potentiated TGFβ1-stimulated signaling activity. Consistent with these findings are our data showing that *Acta2* mRNA levels (which are downstream of TGFβ receptor signaling) in cholesterol-loaded Cav1 knockout VSMCs were

FIGURE 6 Continued

(A) hVSMCs were treated with Chol (5 μg/mL) or 0.2% bovine serum albumin (CT) for 48 hours. qPCR was performed to determine the expression of macrophage marker (*Cd68*) and SMC marker (*Acta2*). (B) hVSMCs were with treated as in A for 48 hours, then qPCR was performed to determine the expression of macrophage differentiation factor *Klf4*. (C) hVSMCs were treated with Chol (5 μg/mL) for the indicated times, then KFL4 expression was determined by Western blotting. (D) *Klf4* (60 nmol/L) or negative CT small, interfering RNA (siRNA) were transfected into hVSMCs for 48 hours. Then, transfected cells were treated as in B, followed by Western blotting for CD68 and KLF4. GAPDH was used as loading CT. (E) Chol-loaded cells (48 hours, 5 μg/mL) were incubated with *Mir145* mimic (60 nmol/L) or CT mimic (60 nmol/LM) for 24 hours and the expressions of CD68, KLF4, and α-SMA determined with GAPDH as a loading CT. The *P* values for the comparisons between CT and *Mir145* mimics are CD68 (0.025), KLF4 (0.018), and α-SMA (0.01). (F-I) hVSMCs were loaded with Chol (48 hours, 5 μg/mL) and were then either treated with HDL (50 μg/mL) for 24 hours or left untreated. Western blotting was performed to determine the expression of (F) KLF4 and (G) CD68. (H) hVSMCs were treated as in F and G, but in the presence or absence of TGFβR1i (50 ng/mL). Western blotting was performed to determine KLF4 expression. For data analysis, unpaired Student's *t*-test was performed for comparing the means of 2 groups. For 2 or more independent groups, 2-way analysis of variance followed by Dunnett post hoc test was performed. Data are presented as the mean ± SEM of at least 3 independent experiments. *P* values are as indicated (*$P < 0.05$, **$P < 0.01$, ***$P < 0.001$, ****$P < 0.0001$). Abbreviations as in Figures 1, 2, and 4.

FIGURE 7 HDL Increases the Expression of *Acta2* Relative to That of CD68 in Atherosclerotic Mice

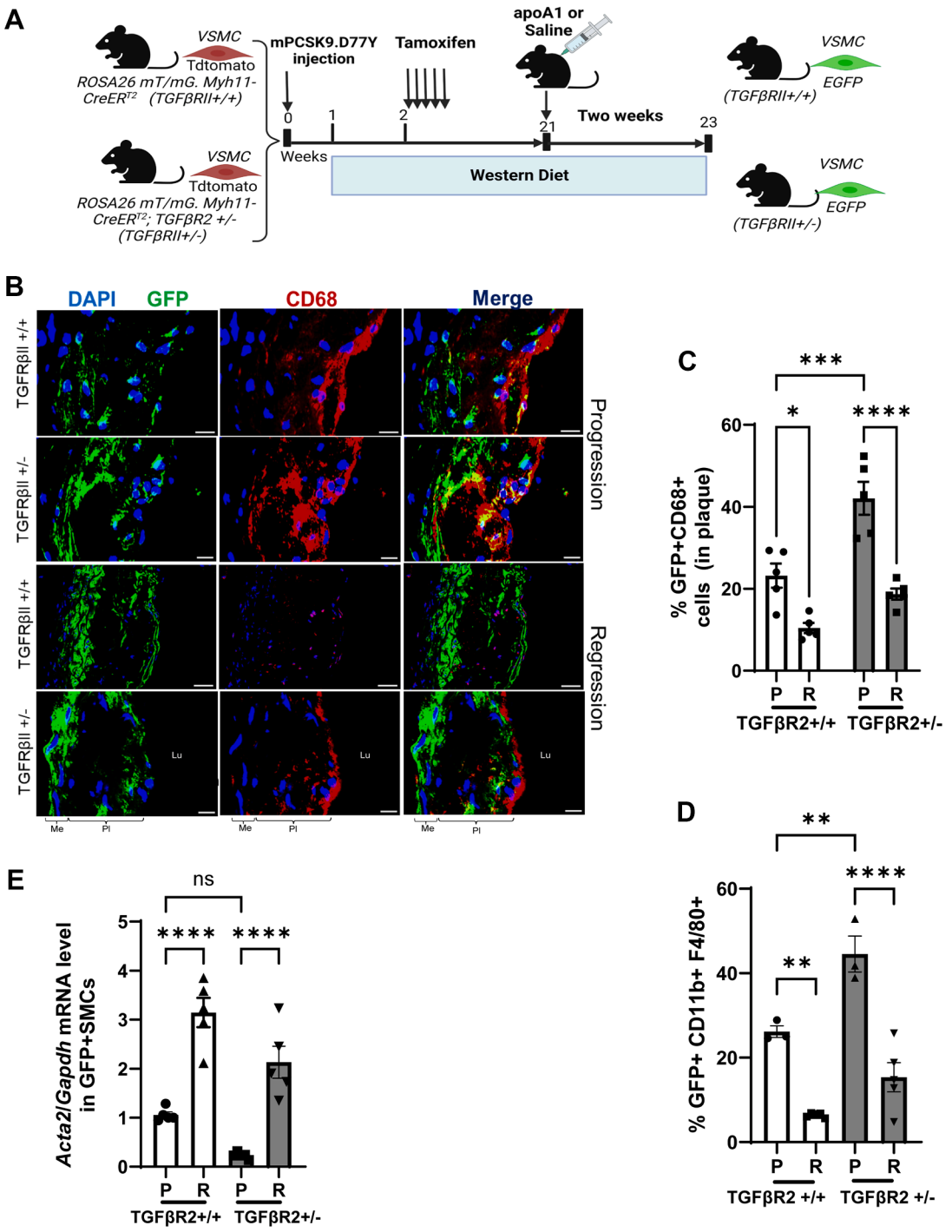

(A) Schematic representation of experimental design. Note that ApoA1, which forms HDL particles in vivo, was injected after atherosclerosis progression (P) to induce regression (R). (B) Representative images from P and R mice that were sufficient (*Tgfβr2*$^{+/+}$) or haplosufficient (*Tgfβr2*$^{+/-}$) for TGFβR2, showing the lineage-positive VSMCs (GFP^{+}) expressing macrophage marker or CD68 (red). Yellow color represents GFP-expressing CD68^{+} cells. (C) Quantification of GFP^{+}/CD68^{+}. (D) Aortic digestion followed by cell sorting of GFP^{+} cells was performed using flow cytometry to capture lineage-positive cells (GFP) expressing macrophage markers (CD11b and F4/80). (E) Total RNA was isolated from sorted cells and qPCR was performed to identify *Acta2* expression. For data analysis of 2 or more independent groups, 2-way analysis of variance followed by Šídák multiple comparisons post hoc test was performed. Data are presented as the mean ± SEM (n = 5-6 mice per group). *P* values are as indicated (*$P < 0.05$, **$P < 0.01$, ***$P < 0.001$, ****$P < 0.0001$). DAPI = 4',6-diamidino-2-phenylindole; other abbreviations as in Figures 1, 2, and 4.

higher than in wild-type cells (Supplemental Figure 5D). Thus, cholesterol efflux, by promoting the displacement of TGFβ receptors from lipid rafts, may increase signaling and downstream gene expression by disrupting the interaction between the receptors and Cav1. Other potential contributions to the changes we observed on signaling after cholesterol-loading, such as effects of HDL and efflux on TGFβ receptor degradation and endocytosis, remain to be investigated in more detail. The similar recoveries of receptors from total cell lysates in cholesterol-loaded and unloaded cells, however, would seem to point away from these possibilities.

We also demonstrate that treatment of cholesterol-loaded hVSMCs with HDL repartitions TGFβRs to nonraft membrane domains, resulting in increased TGFβ-induced downstream signaling and culminating in increased Mir143/145 expression. This restored the contractile phenotype and suppressed KLF4-induced macrophage marker expression. These changes were likely related to the known ability of ApoA1 and HDL to deplete lipid rafts in monocytes and macrophages by promotion of cholesterol efflux,[25,26] which is consistent with finding that HDL did not have significant effects on the expression of Mir143/145 or *Klf4* in ABCA1-deficient mVSMCs.[67] To extend our findings to the in vivo setting, we used a murine model of atherosclerosis with VSMC lineage marking. Consistent with the data in vitro, TGFβR-haplosuffiency increased the proportion in plaques of macrophage marker+ VSMC cells, and ApoA1 injections, which we have previously shown to rapidly deplete plaques of cholesterol,[34] decreased this proportion and increased *Acta2* expression. Furthermore, these changes were associated with evidence that TGFβ signaling was increased in the plaques and the adjacent media.

VSMC-derived macrophage-like cells have been proposed to promote plaque inflammation through a variety of mechanisms[15] and has led to consideration of strategies to revert this phenotype. The results of our studies suggest that ApoA1 or HDL particles can accomplish this, given their success to effect favorable changes in cholesterol-loaded mouse[19,67] or hVSMCs (this study). This would also be consistent with genetic and clinical studies that have found an atheroprotective relationship not with plasma HDL cholesterol levels, but, rather, with the cholesterol efflux function of HDL particles (reviewed in Hewing et al[68]). The results with the treatment of mice with ApoA1 not only extend the in vitro results, but they also suggest that the decreased expression of ABCA1 in intimal VSMCs reported in mouse and human plaques[55,56] does not preclude the benefits of functional HDL in vivo, either because the level we used overcame this deficiency, or that efflux was accomplished by one of the other well-characterized routes of HDL-mediated efflux, such as through ABCG1, aqueous diffusion, or SCARB1.[69] Indeed, studies in vivo have shown that cholesterol flux after administration of HDL particles is preferentially mediated by SCARB1 and ABCG1.[69] Similar to our findings, a recent study[70] highlights the importance of cellular lipid content in determining VSMC phenotypes in atherosclerotic plaques. In their study, Carramolino et al[70] reversed hypercholesterolemia and by studying the fates of lineage-marked VSMCs found that among other changes after lipid lowering in cells that transdifferentiated during atherosclerosis progression were decreases in cellular cholesteryl ester content and increased transcripts of genes with a role in the contractile phenotype, such as *Acta2*.

Because a key consequence of HDL treatment was its induction of *Mir143/145* in cholesterol-loaded hVSMCs, a potential approach to maintaining or restoring the contractile state of VSMCs in atherosclerotic plaques could focus directly on these microRNAs rather than on factors upstream of them. Indeed, there are 2 recent studies in which micelles containing Mir145 were used to treat either hVSMCs isolated from atherosclerotic plaques or mice with atherosclerosis.[41,71] In their study, Cheng et al[71] found that with increasing disease severity, patient-derived hVSMCs had decreasing levels of contractile markers and increasing levels of KLF4. Notably, treatment with *Mir145* micelles rescued contractile marker expression to baseline levels. In the mouse study, treatment with *Mir145* micelles increased mVSMC contractile marker expression, collagen content, and reduced necrotic core in both early atherosclerosis progression and well-established disease.[41] One caveat is that the micelles target CCR2, which, in addition to macrophage-like mVSMCs, would also be expected to result in uptake by monocytes and macrophages.

These results taken with the favorable effects of ApoA1/HDL on TGFβ signaling in vitro and on *Acta2* and CD68 expression in vivo, strengthen the case for therapeutic approaches to boosting of TGFβ signaling if the macrophage-like state is established as deleterious. Besides the present data, such an

FIGURE 8 **HDL Promotes pSMAD2 Levels in TGFβR2$^{+/-}$ Mice In Vivo**

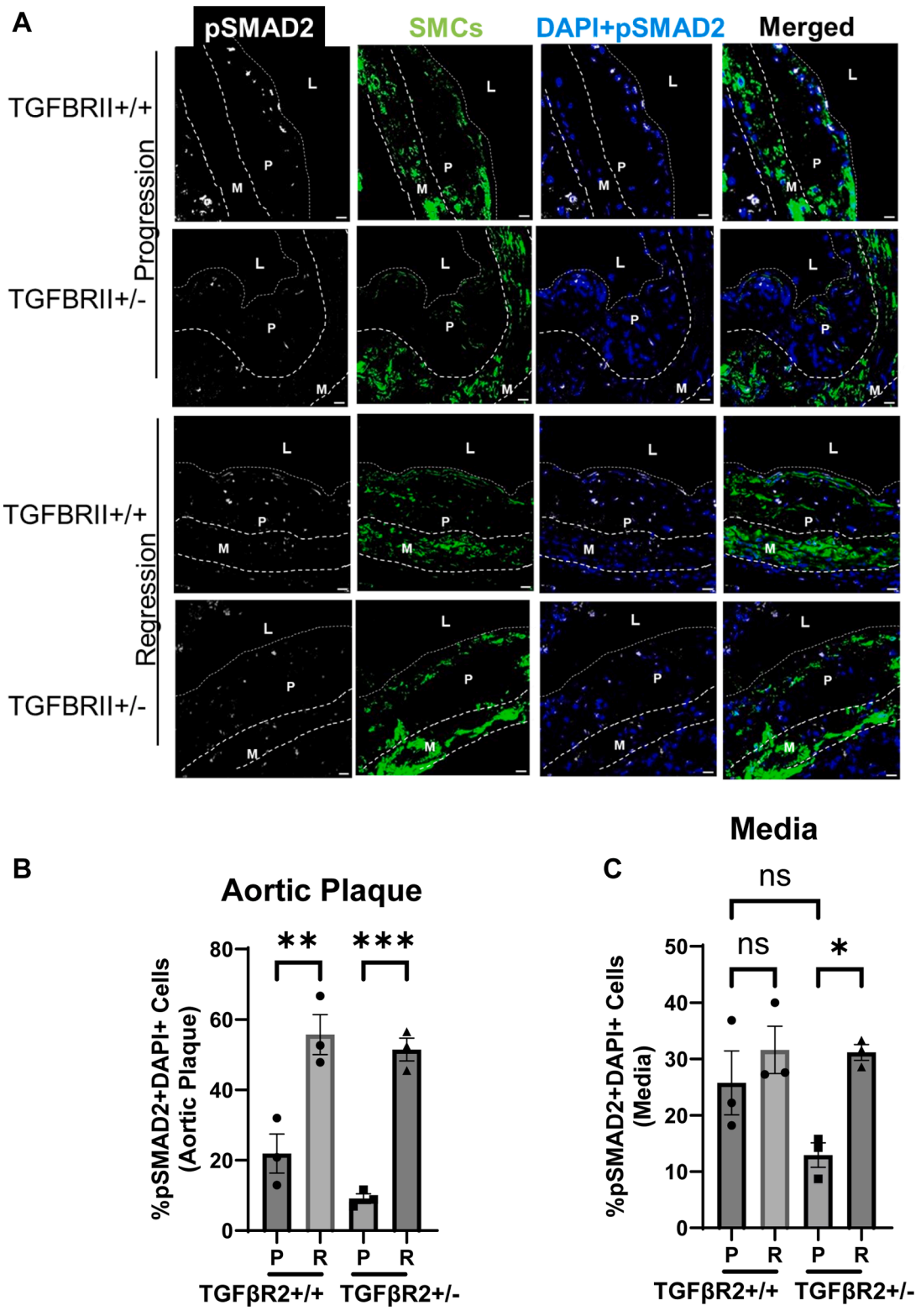

(A) Representative image from P and R mice (TGFβR2$^{+/+}$ and TGFβR2$^{+/-}$) showing the lineage-marked SMCs (GFP^{+} green cells) and pSMAD2 level (white color) (media [M], plaque [P], lumen [L]). pSMAD2^{+} cells were quantified using Image J software in the (B) plaque and (C) media. For data analysis of 2 or more independent groups, 2-way analysis of variance followed by Šídák multiple comparisons post hoc test was performed. Data are presented as the mean ± SEM (n = 3 mice per group). *P* values are as indicated (*$P < 0.05$, **$P < 0.01$, ***$P <$ 0.001). Abbreviations as in Figures 1, 2, and 7.

approach is supported by the growing body of published reports implicating impaired TGFβ signaling in the promotion of vascular disease. For example, deletion of *Tgfβr2* in mVSMCs in *Apoe*$^{-/-}$-deficient mice worsened plaque burden and increased the frequency of phenotypic switching to a macrophage-like cell.[72] In normocholesterolemic mice, the deletion of *Tgfβr2* in VSMCs induced the appearance of macrophage markers in mVSMCs in the mouse aortic wall during aneurysm formation.[16] Additionally, in atherogenic conditions, Smad3 deficiency in mVSMCs promoted chondrogenic and extracellular matrix-remodeling phenotypes.[73] In contrast, mVSMC-specific knockdown of the transcription factor Zeb2 increased the chromatin accessibility of TGFβ signaling mediators and beneficially modulated SMC phenotype.[74]

Whereas the observations from the Simons lab (Chen et al[72]), demonstrating an increase in macrophage-like VSMCs after TGFβ impairment, aligns with the present findings, it should be noted that a report from the Quertermous lab (Cheng et al[74]) found no evidence of a VSMC-derived macrophage-like transition in mouse atherosclerotic plaques. This could be a result of the chosen VSMC model, because we and Chen et al[72] used conditional *Tgfβr2*-deleted mice, whereas Cheng et al[74] conditionally knocked out the downstream mediator Smad3. Because Smad3 may be activated by other pathways (eg, noncanonical TGFβ signaling), this could limit the overlap in the observed phenotypes. Consistent with this are the differences highlighted during murine development, wherein *Tgfβr2*$^{-/-}$ mice are embryonically lethal,[75] but *Smad3*$^{-/-}$ mice are not,[76] suggesting that signaling through these 2 molecules have fundamental differences.

In conclusion, cholesterol-loading promotes hVSMC lipid accumulation, which results in a loss of the contractile and gain of a macrophage-like phenotype by impairing signaling of TGFβ through the partitioning of its receptors to lipid rafts. We also show for the first time that ApoA1/HDL can restore TGFβ signaling in VSMCs in high cholesterol environments not only in vitro, but also in vivo. These results, taken with the literature, collectively suggest that modulating TGFβ signaling in VSMCs within the plaque milieu may be an important target for the development of atheroprotective therapeutics.

STUDY LIMITATIONS. Whereas the data in vitro provide mechanistic evidence for how cholesterol-loading and HDL treatment regulates hVSMC phenotypes, the evidence in vivo is associative, and more direct data will be needed to establish the findings conclusively. More advanced genetic models would benefit such studies, such as the dual lineage approach recently developed using Myh11-Dre and Cd11b-CrexER.[77] In addition, VSMCs can convert to a variety of phenotypes besides a macrophage-like state, including osteoblast-like and fibroblast-like phenotypes within the plaque.[57,74,78-80] Whereas we explored the reversion of macrophage-like VSMCs, future studies should include a variety of phenotypes.

CONCLUSIONS

Our studies highlight the loss of TGFβ signaling and its consequences in VSMCs in a high-cholesterol environment, as well as the therapeutic potential of HDL or ApoA1 to restore VSMC TGFβ signaling to beneficial effect.

ACKNOWLEDGMENTS Dr Nagesh acknowledges his late father Sri Nagesh Thevkar for all his motivation and sacrifice, leading to Dr Nagesh's scientific career, including this manuscript.

FUNDING SUPPORT AND AUTHOR DISCLOSURES

These studies were supported by the following funding: British Heart Foundation (BHF) Centre of Research Excellence grants RE/13/1/30181 and RE/18/3/34214 (to Drs Akbar and Choudhury); BHF Project Grant PG/18/53/33895 to (to Drs Akbar and Choudhury); BHF Intermediate Fellowship FS/IBSRF/22/25110 (to Dr Akbar); National Institutes of Health grants R01HL084312 (to Dr Fisher), and R01HL147476 (to Dr Miano), R01HL138907 (to Dr Sorci-Thomas), and R01HL115141 (to Dr Feinberg); UK-HRI grant UKIG001 (to Dr Misra); and Vanguard Heart Foundation grant NHF1017 (to Dr Misra). All other authors have reported that they have no relationships relevant to the contents of this paper to disclose.

ADDRESS FOR CORRESPONDENCE: Dr Edward A. Fisher, New York University Grossman School of Medicine, SB 705, 435 East 30th Street, New York, New York 10016, USA. E-mail: edward.fisher@nyulangone.org. OR Dr Ashish Misra, Heart Research Institute, 7 Eliza Street, Newtown, New South Wales 2042, Australia. E-mail: ashish.misra@hri.org.au.

PERSPECTIVES

COMPETENCY IN MEDICAL KNOWLEDGE: VSMCs exhibit remarkable phenotypic plasticity in human and mouse atherosclerosis, with estimates of over one-half of macrophage-appearing cells being of VSMC origin. TGFβ signaling is a major regulator of the VSMC contractile state, and in preclinical studies, its loss in VSMCs results in a loss of contractile features and the promotion of a macrophage-like state. It is thought that these cells have adverse effects in atherosclerotic plaques. This is the first study to demonstrate in human coronary artery VSMCs that cholesterol-loading of the cells, as would occur in atherosclerosis progression, down-regulates TGFβ signaling by localizing its receptors into membrane lipid rafts, where they are relatively inactive. Furthermore, cholesterol efflux displaces the receptors from rafts and restores TGFβ signaling, the expression of contractile genes, and the suppression of the macrophage-like state. Similarly, infusion of ApoA1 (which forms cholesterol-efflux competent HDL) into atherosclerotic mice increases the balance between contractile and macrophage features with evidence of increased TGFβ signaling.

TRANSLATIONAL OUTCOMES: The loss of the contractile state and the acquisition of macrophage-like features in arterial VSMCs during atherosclerosis progression is thought to have adverse effects. The present studies not only provide insights into mechanisms and how cholesterol levels can regulate this process, but also highlight a novel potential benefit of functional HDL particles, namely, their ability to protect against the effects of cholesterol-loading on VSMC phenotype, as evidenced in studies in vitro (human coronary artery VSMCs) and in vivo (mice with atherosclerosis). Given the continued interest in HDL-based therapies, the present results may stimulate further efforts for this approach.

REFERENCES

1. Gerrity RG. The role of the monocyte in atherogenesis: II. Migration of foam cells from atherosclerotic lesions. *Am J Pathol*. 1981;103(2):191-200.

2. Trogan E, Feig JE, Dogan S, et al. Gene expression changes in foam cells and the role of chemokine receptor CCR7 during atherosclerosis regression in ApoE-deficient mice. *Proc Natl Acad Sci U S A*. 2006;103(10):3781-3786.

3. Moore KJ, Sheedy FJ, Fisher EA. Macrophages in atherosclerosis: a dynamic balance. *Nat Rev Immunol*. 2013;13(10):709-721.

4. Raghavan S, Singh NK, Gali S, Mani AM, Rao GN. Protein kinase Cθ via activating transcription factor 2-mediated CD36 expression and foam cell formation of Ly6C(hi) cells contributes to atherosclerosis. *Circulation*. 2018;138(21):2395-2412.

5. Robbins CS, Hilgendorf I, Weber GF, et al. Local proliferation dominates lesional macrophage accumulation in atherosclerosis. *Nat Med*. 2013;19(9):1166-1172.

6. Tabas I, Garcia-Cardena G, Owens GK. Recent insights into the cellular biology of atherosclerosis. *J Cell Biol*. 2015;209(1):13-22.

7. Allahverdian S, Chaabane C, Boukais K, Francis GA, Bochaton-Piallat ML. Smooth muscle cell fate and plasticity in atherosclerosis. *Cardiovasc Res*. 2018;114(4):540-550.

8. Doran AC, Meller N, McNamara CA. Role of smooth muscle cells in the initiation and early progression of atherosclerosis. *Arterioscler Thromb Vasc Biol*. 2008;28(5):812-819.

9. Liu M, Gomez D. Smooth muscle cell phenotypic diversity. *Arterioscler Thromb Vasc Biol*. 2019;39(9):1715-1723.

10. Misra A, Feng Z, Chandran RR, et al. Integrin beta3 regulates clonality and fate of smooth muscle-derived atherosclerotic plaque cells. *Nat Commun*. 2018;9(1):2073.

11. Wang Y, Nanda V, Direnzo D, et al. Clonally expanding smooth muscle cells promote atherosclerosis by escaping efferocytosis and activating the complement cascade. *Proc Natl Acad Sci U S A*. 2020;117(27):15818-15826.

12. Feil S, Fehrenbacher B, Lukowski R, et al. Transdifferentiation of vascular smooth muscle cells to macrophage-like cells during atherogenesis. *Circ Res*. 2014;115(7):662-667.

13. Goumans MJ, Ten Dijke P. TGF-β signaling in control of cardiovascular function. *Cold Spring Harb Perspect Biol*. 2018;10(2):a022210.

14. Shi Y, Massagué J. Mechanisms of TGF-beta signaling from cell membrane to the nucleus. *Cell*. 2003;113(6):685-700.

15. Conklin AC, Nishi H, Schlamp F, et al. Meta-analysis of smooth muscle lineage transcriptomes in atherosclerosis and their relationships to in vitro models. *Immunometabolism*. 2021;3(3):e210022.

16. Hu JH, Wei H, Jaffe M, et al. Postnatal Deletion of the Type II Transforming Growth Factor-β Receptor in Smooth Muscle Cells Causes Severe Aortopathy in Mice. *Arterioscler Thromb Vasc Biol*. 2015;35:2647-2656.

17. Chen CL, Liu IH, Fliesler SJ, Han X, Huang SS, Huang JS. Cholesterol suppresses cellular TGF-beta responsiveness: implications in atherogenesis. *J Cell Sci*. 2007;120:3509-3521.

18. Rong JX, Shapiro M, Trogan E, Fisher EA. Transdifferentiation of mouse aortic smooth muscle cells to a macrophage-like state after cholesterol loading. *Proc Natl Acad Sci U S A*. 2003;100(23):13531-13536.

19. Vengrenyuk Y, Nishi H, Long X, et al. Cholesterol loading reprograms the microRNA-143/145-myocardin axis to convert aortic smooth muscle cells to a dysfunctional macrophage-like phenotype. *Arterioscler Thromb Vasc Biol*. 2015;35(3):535-546.

20. Elia L, Quintavalle M, Zhang J, et al. The knockout of miR-143 and -145 alters smooth muscle cell maintenance and vascular homeostasis in mice: correlates with human disease. *Cell Death Differ*. 2009;16(12):1590-1598.

21. Long X, Miano JM. Transforming growth factor-beta1 (TGF-beta1) utilizes distinct pathways for the transcriptional activation of microRNA 143/145 in human coronary artery smooth muscle cells. *J Biol Chem*. 2011;286(34):30119-30129.

22. Cordes KR, Sheehy NT, White MP, et al. miR-145 and miR-143 regulate smooth muscle cell fate and plasticity. *Nature*. 2009;460(7256):705-710.

23. Xu N, Papagiannakopoulos T, Pan G, Thomson JA, Kosik KS. MicroRNA-145 regulates OCT4, SOX2, and KLF4 and represses pluripotency in human embryonic stem cells. *Cell*. 2009;137(4):647-658.

24. Shankman LS, Gomez D, Cherepanova OA, et al. KLF4-dependent phenotypic modulation of smooth muscle cells has a key role in atherosclerotic plaque pathogenesis. *Nat Med*. 2015;21(6):628–637.

25. Murphy AJ, Woollard KJ, Hoang A, et al. High-density lipoprotein reduces the human monocyte inflammatory response. *Arterioscler Thromb Vasc Biol*. 2008;28(11):2071–2077.

26. Iqbal AJ, Barrett TJ, Taylor L, et al. Acute exposure to apolipoprotein A1 inhibits macrophage chemotaxis in vitro and monocyte recruitment in vivo. *Elife*. 2016;5:e15190.

27. Khera AV, Cuchel M, de la Llera-Moya M, et al. Cholesterol efflux capacity, high-density lipoprotein function, and atherosclerosis. *N Engl J Med*. 2011;364(2):127–135.

28. Rohatgi A, Khera A, Berry JD, et al. HDL cholesterol efflux capacity and incident cardiovascular events. *N Engl J Med*. 2014;371(25):2383–2393.

29. Rong JX, Li J, Reis ED, et al. Elevating high-density lipoprotein cholesterol in apolipoprotein E-deficient mice remodels advanced atherosclerotic lesions by decreasing macrophage and increasing smooth muscle cell content. *Circulation*. 2001;104(20):2447–2452.

30. Barrett TJ, Distel E, Murphy AJ, et al. Apolipoprotein AI) promotes atherosclerosis regression in diabetic mice by suppressing myelopoiesis and plaque inflammation. *Circulation*. 2019;140(14):1170–1184.

31. Feig JE, Rong JX, Shamir R, et al. HDL promotes rapid atherosclerosis regression in mice and alters inflammatory properties of plaque monocyte-derived cells. *Proc Natl Acad Sci U S A*. 2011;108(17):7166–7171.

32. Wilhelm AJ, Zabalawi M, Owen JS, et al. Apolipoprotein A-I modulates regulatory T cells in autoimmune LDLr-/-, ApoA-I-/- mice. *J Biol Chem*. 2010;285(46):36158–36169.

33. Li W, Li Q, Jiao Y, et al. Tgfbr2 disruption in postnatal smooth muscle impairs aortic wall homeostasis. *J Clin Invest*. 2014;124(2):755–767.

34. Hewing B, Parathath S, Barrett T, et al. Effects of native and myeloperoxidase-modified apolipoprotein a-I on reverse cholesterol transport and atherosclerosis in mice. *Arterioscler Thromb Vasc Biol*. 2014;34(4):779–789.

35. Akbar N, Digby JE, Cahill TJ, et al. Endothelium-derived extracellular vesicles promote splenic monocyte mobilization in myocardial infarction. *JCI Insight*. 2017;2(17):e93344.

36. Akbar N, Braithwaite AT, Corr EM, et al. Rapid neutrophil mobilization by VCAM-1+ endothelial cell-derived extracellular vesicles. *Cardiovasc Res*. 2023;119(1):236–251.

37. Brown MS, Ho YK, Goldstein JL. The cholesteryl ester cycle in macrophage foam cells: continual hydrolysis and re-esterification of cytoplasmic cholesteryl esters. *J Biol Chem*. 1980;255(19):9344–9352.

38. Abe M, Harpel JG, Metz CN, Nunes I, Loskutoff DJ, Rifkin DB. An assay for transforming growth factor-beta using cells transfected with a plasminogen activator inhibitor-1 promoter-luciferase construct. *Anal Biochem*. 1994;216(2):276–284.

39. Macdonald JL, Pike LJ. A simplified method for the preparation of detergent-free lipid rafts. *J Lipid Res*. 2005;46(5):1061–1067.

40. Chattopadhyay A, Kwartler CS, Kaw K, et al. Cholesterol-induced phenotypic modulation of smooth muscle cells to macrophage/fibroblast-like cells is driven by an unfolded protein response. *Arterioscler Thromb Vasc Biol*. 2021;41(1):302–316.

41. Chin DD, Poon C, Wang J, et al. miR-145 micelles mitigate atherosclerosis by modulating vascular smooth muscle cell phenotype. *Biomaterials*. 2021;273:120810.

42. Chen CL, Huang SS, Huang JS. Cholesterol modulates cellular TGF-beta responsiveness by altering TGF-beta binding to TGF-beta receptors. *J Cell Physiol*. 2008;215(1):223–233.

43. Laping NJ, Grygielko E, Mathur A, et al. Inhibition of transforming growth factor (TGF)-beta1-induced extracellular matrix with a novel inhibitor of the TGF-beta type I receptor kinase activity: SB-431542. *Mol Pharmacol*. 2002;62(1):58–64.

44. Varshney P, Yadav V, Saini N. Lipid rafts in immune signalling: current progress and future perspective. *Immunology*. 2016;149(1):13–24.

45. Stehr M, Estrada CR, Khoury J, et al. Caveolae are negative regulators of transforming growth factor-beta1 signaling in ureteral smooth muscle cells. *J Urol*. 2004;172(6 pt 1):2451–2455.

46. Chen YG. Endocytic regulation of TGF-beta signaling. *Cell Res*. 2009;19(1):58–70.

47. Simons K, Toomre D. Lipid rafts and signal transduction. *Nat Rev Mol Cell Biol*. 2000;1(1):31–39.

48. Kim J, Kim TY, Lee MS, Mun JY, Ihm C, Kim SA. Exosome cargo reflects TGF-β1-mediated epithelial-to-mesenchymal transition (EMT) status in A549 human lung adenocarcinoma cells. *Biochem Biophys Res Commun*. 2016;478(2):643–648.

49. Razani B, Zhang XL, Bitzer M, von Gersdorff G, Böttinger EP, Lisanti MP. Caveolin-1 regulates transforming growth factor (TGF)-beta/SMAD signaling through an interaction with the TGF-beta type I receptor. *J Biol Chem*. 2001;276(9):6727–6738.

50. Pollet H, Conrard L, Cloos AS, Tyteca D. Plasma membrane lipid domains as platforms for vesicle biogenesis and shedding? *Biomolecules*. 2018;8(3):94.

51. Ouweneel AB, Thomas MJ, Sorci-Thomas MG. The ins and outs of lipid rafts: functions in intracellular cholesterol homeostasis, microparticles, and cell membranes: Thematic Review Series: Biology of Lipid Rafts. *J Lipid Res*. 2020;61(5):676–686.

52. Murphy AJ, Woollard KJ, Suhartoyo A, et al. Neutrophil activation is attenuated by high-density lipoprotein and apolipoprotein A-I in in vitro and in vivo models of inflammation. *Arterioscler Thromb Vasc Biol*. 2011;31(6):1333–1341.

53. Boscher C, Nabi IR. Caveolin-1: role in cell signaling. *Adv Exp Med Biol*. 2012;729:29–50.

54. Tellier E, Canault M, Poggi M, et al. HDLs activate ADAM17-dependent shedding. *J Cell Physiol*. 2008;214(3):687–693. https://doi.org/10.1002/jcp.21265

55. Allahverdian S, Chehroudi AC, McManus BM, Abraham T, Francis GA. Contribution of intimal smooth muscle cells to cholesterol accumulation and macrophage-like cells in human atherosclerosis. *Circulation*. 2014;129(15):1551–1559.

56. Wang Y, Dubland JA, Allahverdian S, et al. Smooth muscle cells contribute the majority of foam cells in ApoE (apolipoprotein E)-deficient mouse atherosclerosis. *Arterioscler Thromb Vasc Biol*. 2019;39(5):876–887.

57. Pan H, Xue C, Auerbach BJ, et al. Single-cell genomics reveals a novel cell state during smooth muscle cell phenotypic switching and potential therapeutic targets for atherosclerosis in mouse and human. *Circulation*. 2020;142(21):2060–2075.

58. Feinberg MW, Wara AK, Cao Z, et al. The Kruppel-like factor KLF4 is a critical regulator of monocyte differentiation. *EMBO J*. 2007;26(18):4138–4148.

59. Bjørklund MM, Hollensen AK, Hagensen MK, et al. Induction of atherosclerosis in mice and hamsters without germline genetic engineering. *Circ Res*. 2014;114(11):1684–1689.

60. Miano JM, Fisher EA, Majesky MW. Fate and state of vascular smooth muscle cells in atherosclerosis. *Circulation*. 2021;143(21):2110–2116.

61. Bentzon JF, Otsuka F, Virmani R, Falk E. Mechanisms of plaque formation and rupture. *Circ Res*. 2014;114(12):1852–1866.

62. Bennett MR, Sinha S, Owens GK. Vascular smooth muscle cells in atherosclerosis. *Circ Res*. 2016;118(4):692–702.

63. Basatemur GL, Jorgensen HF, Clarke MCH, Bennett MR, Mallat Z. Vascular smooth muscle cells in atherosclerosis. *Nat Rev Cardiol*. 2019;16(12):727–744.

64. Xie Y, Ostriker AC, Jin Y, et al. LMO7 is a negative feedback regulator of transforming growth factor beta signaling and fibrosis. *Circulation*. 2019;139(5):679–693.

65. Low EL, Baker AH, Bradshaw AC. TGFbeta, smooth muscle cells and coronary artery disease: a review. *Cell Signal*. 2019;53:90–101.

66. Hsiao SC, Liao WH, Chang HA, et al. Caveolin-1 differentially regulates the transforming growth factor-β and epidermal growth factor signaling pathways in MDCK cells. *Biochim Biophys Acta Gen Subj*. 2024;1868(9):130660. https://doi.org/10.1016/j.bbagen.2024.130660

67. Castiglioni S, Monti M, Arnaboldi L, et al. ABCA1 and HDL(3) are required to modulate smooth muscle cells phenotypic switch after cholesterol loading. *Atherosclerosis*. 2017;266:8–15.

68. Hewing B, Moore KJ, Fisher EA. HDL and cardiovascular risk: time to call the plumber? *Circ Res*. 2012;111(9):1117–1120.

69. Cuchel M, Lund-Katz S, de la Llera-Moya M, et al. Pathways by which reconstituted high-density lipoprotein mobilizes free cholesterol from whole body and from

macrophages. *Arterioscler Thromb Vasc Biol*. 2010;30(3):526-532.

70. Carramolino L, Albarrán-Juárez J, Markov A, et al. Cholesterol lowering depletes atherosclerotic lesions of smooth muscle cell-derived fibromyocytes and chondromyocytes. *Nat Cardiovasc Res*. 2024;3(2):203-220. https://doi.org/10.1038/s44161-023-00412-w

71. Patel N, Chin DD, Magee GA, Chung EJ. Therapeutic response of miR-145 micelles on patient-derived vascular smooth muscle cells. *Front Digit Health*. 2022;4:836579.

72. Chen PY, Qin L, Li G, et al. Smooth muscle cell reprogramming in aortic aneurysms. *Cell Stem Cell*. 2020;26(4):542-557.e11.

73. Cheng P, Wirka RC, Kim JB, et al. Smad3 regulates smooth muscle cell fate and mediates adverse remodeling and calcification of the atherosclerotic plaque. *Nat Cardiovasc Res*. 2022;1(4):322-333.

74. Cheng P, Wirka RC, Shoa Clarke L, et al. ZEB2 shapes the epigenetic landscape of atherosclerosis. *Circulation*. 2022;145(6):469-485.

75. Oshima M, Oshima H, Taketo MM. TGF-beta receptor type II deficiency results in defects of yolk sac hematopoiesis and vasculogenesis. *Dev Biol*. 1996;179(1):297-302.

76. Zhu Y, Richardson JA, Parada LF, Graff JM. Smad3 mutant mice develop metastatic colorectal cancer. *Cell*. 1998;94(6):703-714.

77. Li Y, Zhu H, Zhang Q, et al. Smooth muscle-derived macrophage-like cells contribute to multiple cell lineages in the atherosclerotic plaque. *Cell Discov*. 2021;7(1):111.

78. Wirka RC, Wagh D, Paik DT, et al. Atheroprotective roles of smooth muscle cell phenotypic modulation and the TCF21 disease gene as revealed by single-cell analysis. *Nat Med*. 2019;25(8):1280-1289.

79. Kim JB, Zhao Q, Nguyen T, et al. Environment-sensing aryl hydrocarbon receptor inhibits the chondrogenic fate of modulated smooth muscle cells in atherosclerotic lesions. *Circulation*. 2020;142(6):575-590.

80. Alencar GF, Owsiany KM, Karnewar S, et al. Stem cell pluripotency genes Klf4 and Oct4 regulate complex SMC phenotypic changes critical in late-stage atherosclerotic lesion pathogenesis. *Circulation*. 2020;142(21):2045-2059.

KEY WORDS HDL, lipid rafts. TGFβ signaling, vascular smooth muscle cells

APPENDIX For supplemental figures and gels, please see the online version of this paper.